AD-A147 258 HEAT TRANSFER DUE TO FILM CONDENSATION ON VERTICAL FLUTED TUBES(U) NAVAL POSTGRADUATE SCHOOL MONTEREY CA V K GARG ET AL. JUL 84 NPS69-84-006 1/1

UNCLASSIFIED F/G 13/1 NL

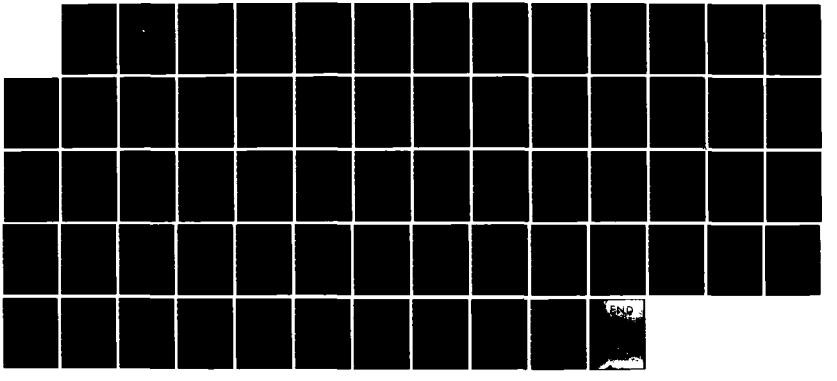

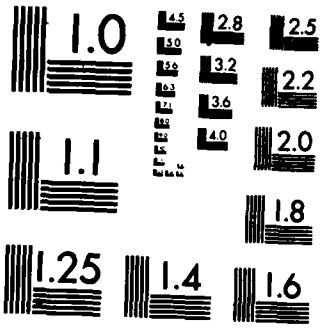
1.0
1.1
1.25
1.4
1.6
1.8
2.0
2.2
2.5
2.8
3.2
3.6
4.0
4.5
5.0
5.6

NPS69-84-006

NAVAL POSTGRADUATE SCHOOL
Monterey, California

HEAT TRANSFER DUE TO FILM CONDENSATION

ON VERTICAL FLUTED TUBES

V. K. Garg
P. J. Marto
July 1984

Final Report for Period
January 1983 - September 1983

Prepared for:

Naval Postgraduate School
Monterey, California 93943

NAVAL POSTGRADUATE SCHOOL
Monterey, California

Commodore R. H. Shumaker
Superintendent

D. A. Schrady
Provost

The work reported herein was supported in part by the Foundation Research Program of the Naval Postgraduate School with funds provided by the Chief of Naval Research.

This report was prepared by:

Vijay K. Garg
Adjunct Professor of
Mechanical Engineering

P. J. Marto
Chairman, Department of
Mechanical Engineering

Reviewed by:

Paul J. Marto
Chairman, Department of
Mechanical Engineering

Released by:

John N. Dyer
Dean of Science and Engineering

Unclassified

SECURITY CLASSIFICATION OF THIS PAGE (When Data Entered)

REPORT DOCUMENTATION PAGE		READ INSTRUCTIONS BEFORE COMPLETING FORM
1. REPORT NUMBER NPS69-84-006	2. GOVT ACCESSION NO. AM7258	3. RECIPIENT'S CATALOG NUMBER
4. TITLE (and Subtitle) Heat Transfer Due to Film Condensation on Vertical Fluted Tubes		5. TYPE OF REPORT & PERIOD COVERED Final Report Jan 83 - Sep 83
		6. PERFORMING ORG. REPORT NUMBER
7. AUTHOR(s) V. K. Garg and P. J. Marto		8. CONTRACT OR GRANT NUMBER(s)
9. PERFORMING ORGANIZATION NAME AND ADDRESS Naval Postgraduate School Monterey, CA 93943		10. PROGRAM ELEMENT, PROJECT, TASK AREA & WORK UNIT NUMBERS
11. CONTROLLING OFFICE NAME AND ADDRESS		12. REPORT DATE July 1984
		13. NUMBER OF PAGES 60
14. MONITORING AGENCY NAME & ADDRESS(if different from Controlling Office)		15. SECURITY CLASS. (of this report) Unclassified
		15a. DECLASSIFICATION/DOWNGRADING SCHEDULE

16. DISTRIBUTION STATEMENT (of this Report)

Approved for public release; distribution unlimited

17. DISTRIBUTION STATEMENT (of the abstract entered in Block 20, if different from Report)

18. SUPPLEMENTARY NOTES

19. KEY WORDS (Continue on reverse side if necessary and identify by block number)

Film Condensation, Fluted Tubes, Surface Tension Forces, Heat Transfer

20. ABSTRACT (Continue on reverse side if necessary and identify by block number)

An analysis of film condensation on a vertical fluted tube has been made considering gravitational and surface tension effects over the entire fluted surface, and using surface-oriented coordinates. For the first time surface tension effects are determined, as they should, from the shape of the condensate-vapor interface rather than the shape of the flute. Two-dimensional conduction within the condensate film as well as in the fluted tube is considered. A finite-difference solution of the highly non-linear

DD FORM 1 JAN 73 1473 EDITION OF 1 NOV 65 IS OBSOLETE

S/N 0102-LF-014-6601

Unclassified

SECURITY CLASSIFICATION OF THIS PAGE (When Data Entered)

20. partial differential equation for the film thickness is coupled with a finite-element solution of the conduction problem. The procedure has been tested on a sinusoidal flute with amplitude to pitch ratio ~0.2. A linear extrapolation, on a log-log basis, of our results shows good comparison with experimental data.

SUMMARY

An analysis of film condensation on a vertical fluted tube has been made considering gravitational and surface tension effects over the entire fluted surface, and using surface-oriented coordinates. For the first time surface tension effects are determined, as they should, from the shape of the condensate-vapor interface rather than the shape of the flute. Two-dimensional conduction within the condensate film as well as in the fluted tube is considered. A finite-difference solution of the highly non-linear partial differential equation for the film thickness is coupled with a finite-element solution of the conduction problem. The procedure has been tested on a sinusoidal flute with amplitude to pitch ratio (approx.) 0.2. A linear extrapolation, on a log-log basis, of our results shows good comparison with experimental data.

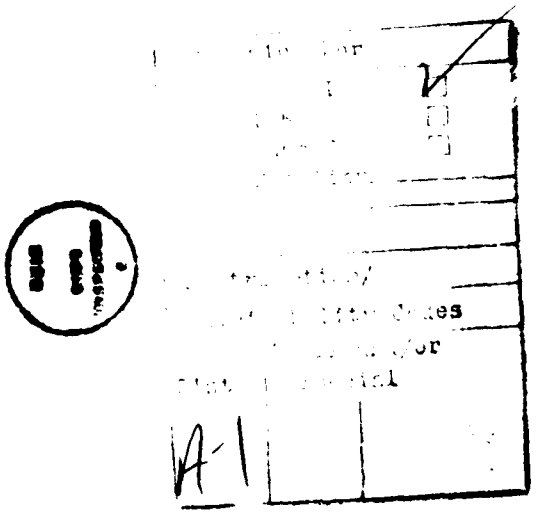

TABLE OF CONTENTS

1. INTRODUCTION

The U.S. Navy has a continued interest in the reduction of the size and weight of propulsion components aboard both surface vessels and submarines. Some studies are currently underway in the Navy to determine the savings in both weight and volume which can occur if the condenser is designed to use corrugated or indented tubing to enhance heat transfer on both the shell and tube sides. While a comprehensive research program has been underway at the Naval Postgraduate School to study various enhancement techniques for horizontal condenser tubes [1,2], an attractive alternative aboard submarines is a vertical condenser oriented aft of the steam turbine as shown in Figure 1(a). With this arrangement, there would be a shorter machinery stack length compared to a horizontal condenser mounted underneath the turbine. This would allow a smaller diameter submarine to be built at a significant reduction in cost. The ultimate aim of this project is therefore to assess the reduction in condenser weight and size that may be feasible if the vertical tubes in this condenser are fluted on the outside (i.e., the steam side), Figure 1(b).

Many methods [3] for enhancing condensation heat transfer have been proposed. Among them, Gregorig [4] first recognized the importance of surface tension in film condensation on vertical fluted tubes. Thereafter, many experimental studies [5-11] on vertical fluted surfaces were made to confirm his findings. Lustenader, et al., [5] employed a fluted vertical tube and obtained about four times larger heat transfer coefficients than those on a vertical smooth tube. Carnavos [6] carried out experiments on a doubly fluted vertical tube and found the augmentation ratio of condensation heat transfer

rate to be about six. Thomas [7,8] tested a vertical tube with longitudinal rectangular fins and wires. The augmentation ratio was about eight. Newson and Hodgson [9] manufactured various condenser tubes of highly enhanced heat transfer performance. Combs and his co-workers [10, 11] at Oak Ridge National Laboratory found the augmentation ratio to be around five for condensation of ammonia and refrigerants on vertical fluted tubes.

Gregorig's theoretical model has also been improved upon but much still remains to be done. Edwards, et al., [12] proposed a condensation model on a heat transfer surface of triangular fins on the assumption of liquid film attaching to the tip of fin with a contact angle. The effect of a locally thin condensate film on the side of the fin (Figure 2) was not considered by them as well as by Fujii and Honda [13]. The latter, however, did consider two-dimensional conduction within the condensate film in the trough region (Figure 2) and within the fin wall. Mori, et al., [14] considered the effect of a thin condensate film on the side of the fin but neglected the variation of its thickness in the vertical direction. They also considered only one-dimensional conduction within the fin and neglected any conduction within the condensate film in the trough region. Hirasawa, et al., [15] improved upon [14] in that they included the variation of a thin condensate film in the vertical direction but neglected conduction within the fin and the film completely. Panchal and Bell [16, 17] also neglected conduction within the fin and the film while analysing a sinusoidal fluted tube, but later found that two-dimensional conduction is important within the fin and the film for a triangular fin [18]. A recent empirical analysis by Barnes and Rohsenow [19], based largely on [16, 20], reports an augmentation ratio of about fifteen for condensation of steam on a fluted surface while most earlier studies

considered condensation of a refrigerant and found much smaller augmentation ratios. With present day knowledge, it is difficult to ascertain whether this discrepancy is due to different fluids or due to a questionable analysis.

All theoretical analyses discussed above break up the fluted surface into basically two parts. In the portion near the crest, gravity is neglected in comparison to the surface tension effect, while in the portion near the trough, the reverse is done. The patching between the two regions is carried out at a point that is selected quite arbitrarily at times [15-18]. This isolation of the two important effects, gravity and surface tension, is justified on the basis that the condensate film is thick in the trough region and thin over the crest. This is, however, not true over the initial portion of the tube length in the vertical direction nor during the initial portion of the tube just below a condensate drainage skirt (Figure 1(b)). These initial portions may be a few pitches in length. A recent analysis by Stack and Merkle [21] does attempt to solve the complete equation with both gravitational and surface tension effects included over the entire flute but has three major drawbacks. First, when the condensate film in the trough region has thickened, the analysis treats it in the boundary-layer-sense, that is, it neglects all velocity gradients except those in the direction normal to the fluted surface. Second, the analysis is restricted to impracticably low values of amplitude to pitch ratio of the flute (0.02 and 0.04) owing to the use of a Cartesian coordinate system rather than a surface-oriented coordinate system. Third, the analysis does not consider any heat transfer effects. Their analysis is only confined to finding the condensate-vapor interface. Fujii and Honda [13] also considered the entire thin film as one piece over an initial length of the tube (about 1/8 of the pitch) but neglected the important surface tension effect.

A major deficiency of all the above theoretical analyses except [21] lies in the way surface tension effect is determined. Contrary to the general belief, this effect does not depend upon the curvature of the condensate-vapor interface. Instead it depends upon the variation of this curvature along the interface. However, since the location of this interface is unknown a priori, many analyses [12, 13] simply determine it on the basis of the known flute shape owing to the argument that in the crest region where the surface tension effect is important, the film is very thin. Such analyses cannot be applied at all to triangular or rectangular fins since their curvature as well as the variation of curvature along the flute is zero. The same is, however, not true for the condensate-vapor interface. Even for sinusoidal flutes, there are large differences between the curvature and its variation along the curved surface for the given flute and the actual interface (see Fig. 10 and its discussion in Section 5). Moreover those analyses that do claim to determine the surface tension effect based on the actual shape of the condensate-vapor interface are also questionable in their claim as shown in Appendix A.

Another problem with all earlier theoretical analyses except [13] is that conduction within the condensate film and the tube wall is either completely neglected or considered to be at most one-dimensional. Panchal and Bell [18] point out clearly that two-dimensional conduction should be considered within both the condensate film and the tube wall.

In an attempt to take care of these deficiencies, an analysis has been developed during this study that solves the complete equation with gravitational as well as surface tension effects included over the entire fluted surface using the surface-oriented coordinate system. In addition, for the first time, surface tension effects are determined as they should, from

the actual shape of the condensate-vapor interface rather than the shape of the flute. Two-dimensional conduction within the condensate film as well as the fluted tube is also included. A finite-difference solution of the highly non-linear partial differential equation for the condensate film thickness is coupled with a finite-element solution of the conduction problem. Details of the analysis follow in subsequent sections.

2. ANALYSIS

Considering the condensate as a viscous, incompressible Newtonian fluid, and setting up a curvilinear orthogonal coordinate system (x_1, x_2, z) as shown in Fig. 3, the continuity equation yields [22]

$$\frac{R}{R + x_2} \frac{\partial u_1}{\partial x_1} + \frac{\partial u_2}{\partial x_2} + \frac{u_2}{R + x_2} + \frac{\partial w}{\partial z} = 0 \quad , \qquad (2.1)$$

where (u_1, u_2, w) are the velocity components in the (x_1, x_2, z) directions respectively, and $R(x_1)$ is the radius of curvature of the fluted tube. The momentum equations are (cf. Ref. 22, p. 68)

x_1-direction:

$$\frac{R}{R+x_2} u_1 \frac{\partial u_1}{\partial x_1} + u_2 \frac{\partial u_1}{\partial x_2} + w \frac{\partial u_1}{\partial z} + \frac{u_1 u_2}{R+x_2} + \frac{1}{\rho} \frac{R}{R+x_2} \frac{\partial p}{\partial x_1}$$

$$= \nu \left[\frac{R^2}{(R+x_2)^2} \frac{\partial^2 u_1}{\partial x_1^2} + \frac{\partial^2 u_1}{\partial x_2^2} + \frac{\partial^2 u_1}{\partial z^2} + \frac{1}{R+x_2} \frac{\partial u_1}{\partial x_2} - \frac{u_1}{(R+x_2)^2} \right.$$

$$\left. + \frac{2R}{(R+x_2)^2} \frac{\partial u_2}{\partial x_1} - \frac{R}{(R+x_2)^3} \frac{dR}{dx_1} u_2 + \frac{Rx_2}{(R+x_2)^3} \frac{dR}{dx_1} \frac{\partial u_1}{\partial x_1} \right] \quad , \qquad (2.2)$$

x_2-direction:

$$\frac{R}{R + x_2} u_1 \frac{\partial u_2}{\partial x_1} + u_2 \frac{\partial u_2}{\partial x_2} + w \frac{\partial u_2}{\partial z} - \frac{u_1^2}{R + x_2} + \frac{1}{\rho} \frac{\partial p}{\partial x_2}$$

$$= \nu \left[\frac{R^2}{(R + x_2)^2} \frac{\partial^2 u_2}{\partial x_1^2} + \frac{\partial^2 u_2}{\partial x_2^2} + \frac{\partial^2 u_2}{\partial z^2} + \frac{1}{R + x_2} \frac{\partial u_2}{\partial x_2} \right.$$

$$\left. - \frac{u_2}{(R+x_2)^2} - \frac{2R}{(R+x_2)^2} \frac{\partial u_1}{\partial x_1} + \frac{R}{(R+x_2)^3} \frac{dR}{dx_1} u_1 + \frac{Rx_2}{(R+x_2)^3} \frac{dR}{dx_1} \frac{\partial u_2}{\partial x_1} \right] , \quad (2.3)$$

z-(vertical) direction:

$$\frac{R}{R + x_2} u_1 \frac{\partial w}{\partial x_1} + u_2 \frac{\partial w}{\partial x_2} + w \frac{\partial w}{\partial z} + \frac{1}{\rho} \frac{\partial p}{\partial z} - \left(1 - \frac{\rho_v}{\rho} \right) g$$

$$= \nu \left[\frac{R^2}{(R+x_2)^2} \frac{\partial^2 w}{\partial x_1^2} + \frac{\partial^2 w}{\partial x_2^2} + \frac{\partial^2 w}{\partial z^2} + \frac{Rx_2}{(R+x_2)^3} \frac{dR}{dx_1} \frac{\partial w}{\partial x_1} + \frac{1}{R+x_2} \frac{\partial w}{\partial x_2} \right] , \quad (2.4)$$

where ρ and ν are the density and kinematic viscosity of the condensate, p is the pressure in the condensate film, g is the acceleration due to gravity, and ρ_v is the density of the vapor.

In order to simplify these equations, we make the usual assumptions that inertia terms are negligible compared to other terms, and that $\partial/\partial x_2 >> \partial/\partial x_1$

or $\partial/\partial z$, and $u_2 << u_1$ or w. This simplifies the momentum equations (2.2) - (2.4) to

$$\frac{\partial^2 u_1}{\partial x_2^2} = \frac{1}{\mu} \frac{R}{R + x_2} \frac{\partial p}{\partial x_1} , \tag{2.5}$$

$$\frac{\partial p}{\partial x_2} = 0 , \tag{2.6}$$

$$\frac{\partial^2 w}{\partial x_2^2} = - \frac{g}{\mu} (\rho - \rho_v) , \tag{2.7}$$

where μ $(=\rho\nu)$ is the dynamic viscosity of the condensate. Integration of (2.7) with boundary conditions

$$\begin{aligned} w &= 0 \text{ at } x_2 = 0 , \\ \mu \frac{\partial w}{\partial x_2} &= S_3 \quad \text{at } x_2 = \delta , \end{aligned} \tag{2.8}$$

yields

$$w = \frac{S_3}{\mu} x_2 + \frac{g}{\mu} (\rho - \rho_v) x_2 \left(\delta - \frac{x_2}{2} \right) . \tag{2.9}$$

Here S_3 is the (known) shear stress (in z-direction) on the condensate-vapor interface, and $\delta(x_1,z)$ is the condensate film thickness. Similarly, integration of (2.5) with boundary conditions

$$\begin{aligned} u_1 &= 0 \quad \text{at} \quad x_2 = 0 \quad , \\ \mu \frac{\partial u_1}{\partial x_2} &= S_1 \quad \text{at} \quad x_2 = \delta \quad , \end{aligned} \tag{2.10}$$

yields

$$u_1 = \frac{S_1}{\mu} x_2 + \frac{R}{\mu} \frac{dp}{dx_1} \left[x_2 \ln \left(\frac{R + x_2}{R + \delta} \right) + R \ln \left(\frac{R + x_2}{R} \right) - x_2 \right] . \tag{2.11}$$

Here S_1 is the (known) shear stress (in x_1-direction) on the condensate-vapor interface.

It is advantageous to use the integral form of the continuity equation rather than the differential form (eqn. (2.1)). We therefore consider the control volume of Fig. 4, and write the continuity equation as

$$\frac{\partial}{\partial x_1} \int_0^\delta u_1 \, dx_2 + \frac{\partial}{\partial z} \int_0^\delta w dx_2 = \frac{k_f}{\rho h_{fg}} \left(\frac{\partial T}{\partial x_2} \right)_{x_2 = \delta} , \tag{2.12}$$

where k_f is the thermal conductivity of the fluid, and h_{fg} is the latent heat of vaporization. The right side of eqn. (2.12) represents the rate at which condensation of vapor takes place. The temperature gradient $\partial T / \partial x_2$ can be

approximated by $(T_s - T_w)/\delta$, where T_s is the saturation temperature at which condensation takes place, and $T_w\,(x_1,z)$ is the wall temperature at $x_2 = 0$. This approximation basically assumes one-dimensional conduction in the condensate film but since $\partial/\partial x_2 \gg \partial/\partial x_1$ or $\partial/\partial z$, and we are interested only in $(\partial T/\partial x_2)_\delta$ at present, it is justifiable to make this approximation.

Substituting for w and u_1 from eqns. (2.9) and (2.11) into eqn. (2.12), and integrating, we get

$$\frac{S_1}{2\mu}\frac{\partial\delta^2}{\partial x_1} + \frac{\delta^2}{2\mu}\frac{\partial S_1}{\partial x_1} - \frac{1}{\mu}\frac{\partial}{\partial x_1}\left[R\,\frac{dp}{dx_1}\left\{\frac{R\delta}{2} + \frac{3\delta^2}{4} - \left(R\delta + \frac{R^2}{2}\right)\cdot \ln\left(1 + \frac{\delta}{R}\right)\right\}\right] + \frac{S_3}{2\mu}\frac{\partial\delta^2}{\partial z} + \frac{\delta^2}{2\mu}\frac{\partial S_3}{\partial z} + \frac{g}{3\mu}(\rho - \rho_v)\frac{\partial\delta^3}{\partial z} = \frac{k_f}{\rho h_{fg}}\,\frac{(T_s - T_w)}{\delta}. \quad (2.13)$$

The pressure p can be related to the surface tension σ and radius of curvature R_i of the condensate vapor interface by

$$p = p_s \pm \sigma/R_i \quad , \quad (2.14)$$

where p_s is the saturation pressure of the vapor. The positive sign holds for $0 \leq x_1 \leq x_p/2$, and the negative sign for $x_p/2 \leq x_1 \leq x_p$, where x_p is the length (curve DE in Fig. 3) along the fluted surface (in x_1-direction) from the crest to the trough (over half the pitch). We are basically interested in analyzing flute shapes that are symmetric about the crest and trough, and therefore take advantage of the symmetry by considering only half of the flute pitch.

Assuming σ to be constant, the pressure gradient may be calculated from eqn. (2.14)

$$\frac{dp}{dx_1} = \pm \sigma \frac{d}{dx_1}\left(\frac{1}{R_i}\right). \tag{2.15}$$

It is thus the variation of curvature of the condensate-vapor interface that is of significance, not the curvature itself. In general, this can be quite different from $d(1/R)/dx_1$, a fact neglected by many previous analyses. Relations for finding $d(1/R_i)/dx_1$ are given in Appendix A.

Equation (2.13) is a partial differential equation for the condensate film thickness $\delta(x_1,z)$. It requires the prior knowledge of shear stresses S_1 and S_3 that come from vapor dynamics and of $T_w(x_1,z)$ that comes from heat conduction analysis for the fluted tube and condensate film. Eqn. (2.13) involves only first order derivatives w.r.t. z but fourth-order derivatives w.r.t. x_1 owing to the presence of dp/dx_1 (cf. eqn. (2.15) and (A-15) or (A-18)). For flute shapes that are symmetric about the crest and trough, the boundary conditions for the solution of eqn. (2.13) are

$$\frac{\partial \delta}{\partial x_1} = \frac{\partial^3 \delta}{\partial x_1^3} = 0 \text{ at } x_1 = 0, \text{ and at } x_1 = x_p \text{ for all } z; \tag{2.16a}$$

$$\delta(x_1,0) = 0.$$

While the boundary condition at z = 0 is correct, it is not practical to start the integration of eqn. (2.13) from z = 0. Therefore, following Stack and Merkle [21], we replace the boundary condition at z = 0 by

$$\delta(x_1,z_0) = \delta_0 \quad , \tag{2.16b}$$

where δ_0 is the film thickness at the initial station z_0, and is found by the classical two-dimensional Nusselt solution

$$\delta_0 = \left\{ \frac{4\mu k_f z_0 (T_s - T_{w00})}{\rho(\rho - \rho_v)\, g h_{fg}} \right\}^{1/4} . \tag{2.17}$$

Here $T_{w00} = T_w(0,z_0) \simeq T_w(0,0)$.

For non-dimensionalization, we take the length L of the vertical fluted tube in the z-direction and length x_p and δ_γ as the characteristic lengths in the x_1, and x_2-directions respectively. Here δ_γ is related to L by the classical Nusselt relation (2.17) in exactly the same manner as δ_0 is related to z_0. Thus, we let

$$\Delta = \delta/\delta_\gamma , \quad X = x_1/x_p , \quad Z = z/L . \tag{2.18}$$

With this non-dimensionalization, eqn. (2.13) and boundary conditions (2.16) can be written as

$$\frac{\partial \Delta^3}{\partial Z} + D_1 \frac{\partial Q}{\partial X} + E_1 \frac{\partial \Delta^2}{\partial X} + E_3 \frac{\partial \Delta^2}{\partial Z} + \Delta^2 \left(\frac{\partial E_1}{\partial X} + \frac{\partial E_3}{\partial Z} \right) = \frac{3D_2}{4\Delta} , \tag{2.19}$$

$$\frac{\partial \Delta}{\partial X} = \frac{\partial^3 \Delta}{\partial X^3} = 0 \quad \text{at } X = 0,1 \text{ for all } Z, \tag{2.20a}$$

$$\Delta(X,Z_0) = Z_0^{1/4} , \tag{2.20b}$$

where

$$Z_0 = z_0/L \ ,$$

$$D_1 = \frac{3\sigma L}{g(\rho-\rho_v)\, x_p\, \delta_\gamma^2} \ ,$$

$$D_2 = \frac{T_s - T_w}{T_s - T_{w00}} \ ,$$

$$E_1 = \frac{3LS_1}{2g\,(\rho-\rho_v)x_p\delta_\gamma} \ ,$$

$$E_3 = \frac{3S_3}{2g(\rho-\rho_v)\delta_\gamma} \ ,$$

$$Q = R_c\left[R_c\,\Delta/2 + 3\,D_3\,\Delta^2/4 - (R_c\Delta + R_c^2/2D_3)\,\ln\,(1+D_3\Delta/R_c)\right]F \ ,$$

$$D_3 = \delta_\gamma/x_p \ ,$$

$$R_c = R/x_p \ ,$$

$$F = \pm\,\frac{d}{dX}\left(\frac{1}{R_n}\right) = \pm\, x_p^2\,\frac{d}{dx_1}\left(1/R_i\right) \ , \qquad \begin{cases} - \text{ for } 0 < X < 1/2 \\ + \text{ for } 1/2 < X < 1 \end{cases} \ ,$$

and

$$R_n = R_i/x_p$$

Equation (2.19) is a highly non-linear partial differential equation. It is solved numerically by the finite-difference technique as detailed below.

3. FINITE-DIFFERENCE METHOD

Equation (2.19) is parabolic in Z so that a forward marching scheme in the Z-direction can be used. Thus the choice of δ_0 will affect only the region near z_0, and its effect will die out as z increases. This was indeed found to be true. Equation (2.19) as written is in conservative form. An equivalent but non-conservative form can be obtained by expanding the derivatives in (2.19) and dividing by $3\Delta^2$. In that non-conservative form, the equation is still parabolic in Z but the mass is <u>not</u> identically conserved when the equation is integrated <u>numerically</u> [21].

We divide the interval $0 \leq X \leq 1$ into n equal parts. Taking δX and δZ as the step sizes in X and Z-directions respectively, and using backward differencing in Z and mixed differencing in X-direction, we write the finite-difference form of eqn. (2.19) as

$$\frac{\Delta^3_{i,k} - \Delta^3_{i,k-1}}{(\delta Z)} + D_1 \frac{\beta Q_{i+1,k} + (1-2\beta)Q_{i,k} - (1-\beta)Q_{i-1,k}}{(\delta X)}$$

$$+ E_1 \frac{\beta\Delta^2_{i+1,k} + (1-2\beta)\Delta^2_{i,k} - (1-\beta)\Delta^2_{i-1,k}}{(\delta X)} + E_3 \frac{\Delta^2_{i,k} - \Delta^2_{i,k-1}}{(\delta Z)}$$

$$+ \Delta^2_{i,k} \left(\frac{\partial E_1}{\partial X} + \frac{\partial E_3}{\partial Z} \right) = \frac{3D_2}{4\Delta_{i,k}} , \qquad (3.1)$$

where the subscripts i and k represent the location in X and Z directions respectively (cf. Fig. 5), and β is a number that is selected between 0 and 1; $\beta = 0$ corresponds to backward differencing, $\beta = 1$ to forward differencing, and $\beta = 1/2$ to central differencing in X. Since eqn. (2.20b) gives Δ's for all X (i.e., for all i) at Z_0 (say k = 1), we can march forward in the Z-direction. In other words, Δ's at (k-1) for all i are known in eqn. (3.1). Thus (3.1) leads to a tridiagonal set of non-linear algebraic equations to be solved for (n+1) values of Δ's at each location k of forward march in the Z-direction. This non-linear set is solved by linearization and successive iteration. Let us write eqn. (3.1) in the form

$$A_i\left(\Delta_{i-1,k}\right)^m + B_i\left(\Delta_{i,k}\right)^m + C_i\left(\Delta_{i+1,k}\right)^m = R_i \quad , \qquad (3.2)$$

where $(\ )^m$ represents the values at the (current) mth iteration, and the coefficients A_i, B_i, C_i, and R_i depend upon the method of linearization.

For linearization three methods were tried. In the first method, we simply let

$$\left(\Delta^{\,j}_{i,k}\right)^m = \left(\Delta^{\,j-1}_{i,k}\right)^{m-1}\left(\Delta_{i,k}\right)^m \quad , \quad j = 1,2,3, \qquad (3.3)$$

where $(\ )^{m-1}$ represents the known values at the (previous) (m-1)th iteration. The iteration is started by taking $\Delta_{i,k} = \Delta_{i,k-1}$ for all i. With this linearization the coefficients in eqn. (3.2) are

$$A_i = -\frac{\delta Z}{\delta X}(1-\beta)\left[D_1\left(G_{i-1,k}\right)^{m-1} + E_1\left(\Delta_{i-1,k}\right)^{m-1}\right],\ i = 1,2,\ldots,(n-1) \quad (3.4a)$$

$$B_i = \left(\Delta_{i,k}\right)^{m-1}\left[\left(\Delta_{i,k}\right)^{m-1} + E_3 + \delta Z\left(\frac{\partial E_1}{\partial X} + \frac{\partial E_3}{\partial Z}\right)_{i,k}\right]$$

$$+ \frac{\delta Z}{\delta X}(1-2\beta)\left[D_1\left(G_{i,k}\right)^{m-1} + E_1\left(\Delta_{i,k}\right)^{m-1}\right],\ i = 0,1\ldots,n \quad (3.4b)$$

$$C_i = \frac{\delta Z}{\delta X}\beta\left[D_1\left(G_{i+1,k}\right)^{m-1} + E_1\left(\Delta_{i+1,k}\right)^{m-1}\right],\quad i = 1,2,\ldots,(n-1) \quad (3.4c)$$

$$R_i = \Delta_{i,k-1}^3 + E_3\,\Delta_{i,k-1}^2 + \frac{3D_2(\delta Z)}{4\left(\Delta_{i,k}\right)^{m-1}},\ i = 0,1,\ldots,n \quad (3.4d)$$

$$A_n = -\frac{\delta Z}{\delta X}\left[D_1\left(G_{n-1,k}\right)^{m-1} + E_1\,(1-2\beta)\left(\Delta_{n-1,k}\right)^{m-1}\right], \quad (3.4e)$$

$$C_0 = \frac{\delta Z}{\delta X}\left[D_1\left(G_{1,k}\right)^{m-1} - E_1(1-2\beta)\left(\Delta_{1,k}\right)^{m-1}\right], \quad (3.4f)$$

where

$$G = R_c\left[R_c/2 + 3D_3\Delta/4 - \left(R_c + \frac{R_c^2}{2\,D_3\,\Delta}\right)\ln\left(1 + D_3\Delta/R_c\right)\right] \quad F = Q/\Delta, \quad (3.4g)$$

and the boundary conditions in (2.20a) have been taken into account. This method works but has two drawbacks. Its convergence is slow, and it requires heavy under-relaxation for convergence. The latter implies that it is necessary to under-relax the values of Δ after every iteration according to

$$(\Delta)^m = (\Delta)^{m-1} + \lambda \left[(\Delta)^m - (\Delta)^{m-1} \right] \quad , \qquad (3.5)^*$$

where the relaxation factor $\lambda < 1$. In fact, it was found that λ decreases from about 0.5 at Z_0 to very small values as Z increases. Typically $\lambda < 0.1$ for $Z > 0.02$.

In the second method, we used Taylor series expansion in order to linearize terms containing Δ^2 and Δ^3. Thus we let

$$\left(\Delta^3_{i,k} \right)^m = 3 \left(\Delta^2_{i,k} \right)^{m-1} \left(\Delta_{i,k} \right)^m - 2 \left(\Delta^3_{i,k} \right)^{m-1} \quad , \qquad (3.6a)$$

and

$$\left(\Delta^2_{i,k} \right)^m = 2 \left(\Delta_{i,k} \right)^{m-1} \left(\Delta_{i,k} \right)^m - \left(\Delta^2_{i,k} \right)^{m-1} \quad . \qquad (3.6b)$$

With this linearization the coefficients in eqn. (3.2) are

$$A_i = - \frac{\delta Z}{\delta X} (1-\beta) \left[D_1 \left(G_{i-1,k} \right)^{m-1} + 2 E_1 \left(\Delta_{i-1,k} \right)^{m-1} \right], \quad i=1,2,\ldots,(n-1) \qquad (3.7a)$$

---

* This equation is to be treated in the context of an equivalent FORTRAN statement.

$$B_i = \left(\Delta_{i,k}\right)^{m-1}\left[3\left(\Delta_{i,k}\right)^{m-1} + 2E_3 + 2(\delta Z)\left(\frac{\partial E_1}{\partial X} + \frac{\partial E_3}{\partial Z}\right)_{i,k}\right]$$

$$+ \frac{\delta Z}{\delta X}(1-2\beta)\left[D_1\left(G_{i,k}\right)^{m-1} + 2E_1\left(\Delta_{i,k}\right)^{m-1}\right], \quad i = 0,1,\ldots,n \qquad (3.7b)$$

$$C_i = \frac{\delta Z}{\delta X}\beta\left[D_1\left(G_{i+1,k}\right)^{m-1} + 2E_1\left(\Delta_{i+1,k}\right)^{m-1}\right], \quad i = 1,2,\ldots(n-1) \qquad (3.7c)$$

$$R_i = \Delta^3_{i,k-1} + E_3\,\Delta^2_{i,k-1} + \frac{3D_2(\delta Z)}{4\left(\Delta_{i,k}\right)^{m-1}} + 2\left(\Delta^3_{i,k}\right)^{m-1}$$

$$+ E_1\frac{\delta Z}{\delta X}\left[\beta\left(\Delta^2_{i+1,k}\right)^{m-1} + (1-2\beta)\left(\Delta^2_{i,k}\right)^{m-1} - (1-\beta)\left(\Delta^2_{i-1,k}\right)^{m-1}\right]$$

$$+\left[E_3 + \delta Z\left(\frac{\partial E_1}{\partial X} + \frac{\partial E_3}{\partial Z}\right)_{i,k}\right]\left(\Delta^2_{i,k}\right)^{m-1}, \quad i=1,2,\ldots,(n-1) \qquad (3.7d)$$

$$A_n = -\frac{\delta Z}{\delta X}\left[D_1\left(G_{n-1,k}\right)^{m-1} + 2E_1(1-2\beta)\left(\Delta_{n-1,k}\right)^{m-1}\right], \qquad (3.7e)$$

$$C_0 = \frac{\delta Z}{\delta X}\left[D_1\left(G_{1,k}\right)^{m-1} - 2E_1(1-2\beta)\left(\Delta_{1,k}\right)^{m-1}\right], \qquad (3.7f)$$

$$R_0 = \Delta^3_{0,k-1} + E_3\,\Delta^2_{0,k-1} + \frac{3D_2(\delta Z)}{4\left(\Delta_{0,k}\right)^{m-1}} - E_1\,\frac{\delta Z}{\delta X}\,(1-2\beta)\left(\Delta^2_{1,k}\right)^{m-1}$$

$$+\left(\Delta^2_{0,k}\right)^{m-1}\left[2\left(\Delta_{0,k}\right)^{m-1} + E_1\,\frac{\delta Z}{\delta X}\,(1-2\beta) + E_3 + \delta Z\left(\frac{\partial E_1}{\partial X} + \frac{\partial E_3}{\partial Z}\right)_{0,k}\right], \qquad (3.7g)$$

$$R_n = \Delta^3_{n,k-1} + E_3\,\Delta^2_{n,k-1} + \frac{3D_2(\delta Z)}{4\left(\Delta_{n,k}\right)^{m-1}} - E_1\,\frac{\delta Z}{\delta X}\,(1-2\beta)\left(\Delta^2_{n-1,k}\right)^{m-1}$$

$$+\left(\Delta^2_{n,k}\right)^{m-1}\left[2\left(\Delta_{n,k}\right)^{m-1} + E_1\,\frac{\delta Z}{\delta X}\,(1-2\beta) + E_3 + \delta Z\left(\frac{\partial E_1}{\partial X} + \frac{\partial E_3}{\partial Z}\right)_{n,k}\right], \qquad (3.7h)$$

where G is again given by (3.4g) and the boundary conditions in (2.20a) have been accounted for.

It is of interest to note from eqns. (3.7) that the Taylor series expansion was <u>not</u> used to linearize the right side of eqn. (3.1) as well as the terms involving Q on the left side of (3.1). While such a linearization of the right side of (3.1) can be carried out without much difficulty, it was not found to be beneficial. The unnecessary complication was therefore avoided. The Taylor series linearization of terms involving Q in (3.1) was also tried but was found not to work at all. This method was found to be the best of the three. It allows a larger step size (δZ) in the Z-direction, and

a larger relaxation factor λ than the first method. Overall, it is better than the first method by a factor of at least twenty, and was therefore adopted. The third method consisted in the use of Newton-Raphson method for solution of the non-linear equations. A general outline of this method is given in Appendix B. Though this method does not require any relaxation factor, it produced absurd results (Δ's oscilling with X after a few step sizes in the Z-direction), and was therefore abandoned.

4. COMPUTATIONAL DETAILS

Before the set of equations (3.2) resulting from eqn.(3.1) can be solved, we need to specify values of the dimensionless parameters E_1, E_3 and D_2. This requires the prior knowledge of shear stresses $S_1$and S_3, and the temperature $T_w(x_1, z)$ of the condensate-wall interface. The computer code does have the provision for specification of shear stresses S_1 and S_3 but for the present results both these stresses were set to zero. This is because vapor dynamics that determines these stresses is beyond the scope of the present work. The computer code, however, does calculate $T_w(x_1,z)$ by considering two-dimensional conduction within the fluted tube as well as the condensate film. For this, the Laplace equation

$$k\left(\frac{\partial^2 T}{\partial x^2} + \frac{\partial^2 T}{\partial y^2}\right) = 0 \qquad (4.1)$$

is solved subject to the boundary conditions

$$\frac{\partial T}{\partial x} = 0 \text{ at } x = 0,\ P/2 \text{ where } P = \text{pitch of the flute,}$$

$$T = T_s \text{ at the vapor-condensate interface,} \qquad (4.2)$$

$$\text{and} \quad T = T_c \text{ at the coolant-tube interface,}$$

where k is the thermal conductivity, and T_c is the coolant temperature assumed to vary linearly from the coolant inlet to exit temperature. The last boundary condition in (4.2) needs modification due to a film resistance on the coolant side but such a specification either requires an ad-hoc value of the film resistance or a consideration of coolant dynamics that was also considered beyond the scope of the present analysis. Solution of eqns. (4.1) and (4.2) was obtained by a finite element method in which the region OABCO

(Fig.3) was divided into several linear triangular elements. Details for this can be found in any text on the finite element method. Some care is, however, required since the thermal conductivity of the fluid in region ABEDA is vastly different from that of the tube material in region DECOD (Fig.3). The finite element method was preferred over the finite-difference method owing to the irregular shape of surface AB (Fig. 3). From this solution, we get the values of $T_w(x_1,z)$ on the surface DE (Fig.3).

Since the solution of eqn. (3.1) requires $T_w(x_1,z)$ which comes from the solution of (4.1) for which knowledge of δ-values is essential (for locating surface AB in Fig.3), the two solutions are coupled. Also, since the solution of (3.1) is found iteratively, it implies that eqn.(4.1) should be solved at every iteration. This places a rather prohibitive demand on the computer time. However, since (δZ) is small, of the order of 10^{-5}, changes in δ are small at every iteration with the result that it is not really necessary to solve equation (4.1) at every iteration. Thus (4.1) was solved only once per step in the Z-direction. This saves considerable computer time since the finite element solution of (4.1) requires almost as much computer time as nearly one hundred iterations for solution of (3.1). Some sample runs were initially made to confirm that the error in δ-values due to this time saving feature was really negligible.

4.1 Condensate-Vapor Interface Profile

As pointed out in Appendix A, one method for finding $d(1/R_i)/dx_1$ is by use of equation (A.8) which involves derivatives of $f_i(x)$, where $f_i(x)$ describes the condensate-vapor interface at any Z. Several methods were used to find these derivatives but none of them proved worthwhile since $f_i(x)$ is known at unequally-spaced values of x. The methods are listed below for the sake of completeness.

i) Cubic splines were fitted in a least squares manner through f_i values to find f_i' and f_i''. Then cubic splines were fitted through the previously computed f_i' values to find f_i'''. A slight variation of this method was to fit cubic splines repeatedly through f_i, f_i' and f_i'' values to find f_i'''. Both these methods gave different values for f_i'' and f_i''' pointing to their futility.

ii) Parabolas were fitted through three consecutive points in succession on the condensate-vapor interface, and R_i and $d(1/R_i)/dx_1$ were computed at the point central to each set of three points. This also led to inconsistent results.

iii) An attempt to fit a truncated Fourier series (having 3-4 terms) through f_i values was made. This was attempted since we were working with a sinusoidal flute. However, since the fit itself was poor, no attempt was made to calculate the derivatives. A better fit (Fig. 6) was obtained by fitting $(a_1 + a_2 \cos 2\pi x/P)$ through all (n+1) values of f_i, where the coefficients a_1 and a_2 were found for a least squares fit. However, even this fit was considered inadequate to find $d(1/R_i)/dx_1$. A slight variation of this was to fit $(a_1 + a_2 \cos 2\pi x/P)$ through the first n/2 values of f_i (for $x < P/2$) and a similar curve through the last n/2 values. This produced a very good fit on visual inspection (Fig.7). However, using it to find $d(1/R_i)/dx_1$ leads to wiggles in δ-values. Solution of equations (3.1) and (4.1) starting from Z_o leads to film shape rising suddenly in the trough region (Fig.8) after a few (δZ) steps, thus violating the boundary conditions there. Starting from $Z = 0.07$, with results at $Z = 0.07$ found by better methods, the solution leads to such large wiggles that even negative values of δ are found only a few steps downstream. In an effort to improve upon this situation, values of δ were computed to correspond to the fit in Fig. 7 before iterating. This,

however, slowed down the convergence so much that even two hundred iterations were insufficient for the same tolerance. In fact, it appeared as if convergence would never take place. Nevertheless, this exercise did point out the reason for the failure of the above technique, since the differences between the original δ-values and those conforming to the good (!) fit in Fig. 7 were found to be large, as much as 20%.

iv) Efforts to use lagrangian interpolation to compute f_i values at equi-distant x values, and then use techniques described in Section 4.2 to find f_i', etc. also produced absurd results. Use of equation (A.8) to compute $d(1/R_i)/dx_1$ was therefore abandoned.

It may be mentioned that while using eqn. (I.8) to find $d(1/R_i)/dx_1$, a futile attempt was also made to solve the partial differential equation (2.13) directly in terms of δ^3 rather than δ.

4.2 Derivatives of Condensate Film Thickness

Use of either eqn. (A.15) or (A.18) to find $d(1/R_i)/dx_1$ requires the determination of first three derivatives of δ w.r.t. x_1. Fortunately δ is known at equidistant values of x_1. It is therefore easier to find these derivatives than those of f_i w.r.t. x. Several methods for this determination were also tried with varying degrees of success.

i) Derivatives of delta were found by fitting a cosine to the vapor-condensate interface in a manner analogous to that described in Sec. 4.1, but it resulted in absolutely useless results.

ii) Another fruitless effort was to fit least squares cubic splines, repeatedly or otherwise, through δ-values so as to find δ', δ'' and δ'''.

iii) The first derivative of δ w.r.t. x_1 was found by solving the following set of linear equations [23, p.56]:

$$\delta'_{i-1} + 4\delta'_i + \delta'_{i+1} = \frac{6}{\delta x_1}\left(\delta_{i+1} - \delta_{i-1} \right) \quad , i = 1,2,\ldots,(n-1),$$

$$\delta'_o = 0 \quad , \quad \delta'_n = 0 \quad , \quad \delta x_1 = x_p(\delta X), \tag{4.3}$$

and the second derivative, δ'', by solving

$$\delta''_{i-1} + 10\delta''_i + \delta''_{i+1} = \frac{12}{(\delta x_1)^2}\left(\delta_{i-1} - 2\delta_i + \delta_{i+1} \right), \quad i=1,2,\ldots,(n-1),$$

$$5\delta''_o + \delta''_1 = \frac{12}{(\delta x_1)^2}\left(\delta_1 - \delta_o \right), \tag{4.4}$$

$$\delta''_{n-1} + 5\delta''_n = \frac{12}{(\delta x_1)^2}\left(\delta_{n-1} - \delta_n \right).$$

Though these sets of linear equations are tridiagonal and can be solved easily, they do represent an increase in computer time. Besides the method yields rather poor results.

iv) A method that gives better results than those obtained by above methods is based on passing least squares quartics through seven consecutive points at a time. Leaving the details to the reader (see also [24], p.492), we present the equations for finding δ_i', δ_i'' and δ_i''' for i = o, 1,..., n. These equations make use of the boundary conditions (2.16a), and the fact that δ is known at equidistant x_1 values.

Relations for δ', accurate to $O(\delta x)^4$, are

$$\delta_i' = \left(22\delta_{i-3} - 67\delta_{i-2} - 58\delta_{i-1} + 58\delta_{i+1} + 67\delta_{i+2} - 22\delta_{i+3}\right)/ 252\delta x_1 ,$$

$$i = 3,4,\ldots,(n-3),$$

$$\delta_o' = 0 \quad , \quad \delta_n' = 0,$$

$$\delta_1' = \left(-58\delta_o - 67\delta_1 + 80\delta_2 + 67\delta_3 - 22\delta_4\right)/ 252\delta x_1 ,$$

$$\delta_2' = \left(-67\delta_o - 36\delta_1 + 58\delta_3 + 67\delta_4 - 22\delta_5\right)/ 252\delta x_1 , \qquad (4.5)$$

$$\delta_{n-2}' = \left(22\delta_{n-5} - 67\delta_{n-4} - 58\delta_{n-3} + 36\delta_{n-1} + 67\delta_n\right)/ 252\delta x_1 ,$$

and

$$\delta_{n-1}' = \left(22\delta_{n-4} - 67\delta_{n-3} - 80\delta_{n-2} + 67\delta_{n-1} + 58\delta_n\right)/ 252\delta x_1 .$$

Relations for δ'', accurate to $O(\delta x_1)^4$, are

$$\delta_i'' = \left(-13\delta_{i-3} + 67\delta_{i-2} - 19\delta_{i-1} - 70\delta_i - 19\delta_{i+1} + 67\delta_{i+2} - 13\delta_{i+3}\right) / 132\delta x_1^2 ,$$

$$i = 3,4,\ldots,(n-3),$$

$$\delta_o'' = \left(-26\delta_3 + 134\delta_2 - 38\delta_1 - 70\delta_o\right) / 132\delta x_1^2 ,$$

$$\delta_1'' = \left(-13\delta_4 + 67\delta_3 - 32\delta_2 - 3\delta_1 - 19\delta_o\right) / 132\delta x_1^2 ,$$

$$\delta_2'' = \left(-13\delta_5 + 67\delta_4 - 19\delta_3 - 70\delta_2 - 32\delta_1 + 67\delta_o\right) / 132\delta x_1^2 , \qquad (4.6)$$

$$\delta_{n-2}'' = \left(-13\delta_{n-5} + 67\delta_{n-4} - 19\delta_{n-3} - 70\delta_{n-2} - 32\delta_{n-1} + 67\delta_n\right) / 132\delta x_1^2 ,$$

$$\delta_{n-1}'' = \left(-13\delta_{n-4} + 67\delta_{n-3} - 32\delta_{n-2} - 3\delta_{n-1} - 19\delta_n\right) / 132\delta x_1^2 ,$$

and

$$\delta_n'' = \left(-26\delta_{n-3} + 134\delta_{n-2} - 38\delta_{n-1} - 70\delta_n\right) / 132\delta x_1^2 .$$

Relations for δ''' are

$$\delta'''_i = \left(- \delta_{i-3} + \delta_{i-2} + \delta_{i-1} - \delta_{i+1} - \delta_{i+2} + \delta_{i+3} \right) / \; 6 \; \delta x_1^3 \quad ,$$

$$i = 3,4,\ldots,(n-3),$$

$$\delta'''_o = 0 \; , \; \delta'''_n = 0 \; ,$$

$$\delta'''_1 = \left(\delta_4 - \delta_3 - 2\delta_2 + \delta_1 + \delta_o \right) / \; 6 \; \delta x_1^3 \quad , \tag{4.7}$$

$$\delta'''_2 = \left(\delta_5 - \delta_4 - \delta_3 + \delta_o \right) / \; 6 \delta x_1^3 \quad ,$$

$$\delta'''_{n-2} = \left(- \delta_{n-5} + \delta_{n-4} + \delta_{n-3} - \delta_n \right) / \; 6 \; \delta x_1^3 \quad ,$$

and

$$\delta'''_{n-1} = \left(- \delta_{n-4} + \delta_{n-3} + 2 \; \delta_{n-2} - \delta_{n-1} - \delta_n \right) / \; 6 \; \delta x_1^3 \quad .$$

Use of these equations for finding δ', δ'' and δ''' leads to mild fluctuations in δ-values after a few steps in the Z-direction. Their use had, therefore, to be abandoned. Less accurate relations involving an error of $0\ \delta_1^2$ also yielded similar results.

v) The best method for finding the derivatives of δ for this problem turned out to be the use of central difference formulae

$$\delta_i' = \left(\delta_{i+1} - \delta_{i-1}\right) / \ 2\ \delta x_1 \quad , \quad i = 1,2,\ldots,(n-1) \quad ,$$
$$\delta_o' = \delta_n' = 0 \quad , \tag{4.8}$$

for the first derivative, and

$$\delta_i'' = \left(\delta_{i+1} - 2\ \delta_i + \delta_{i-1}\right) / \ \delta x_1^2 \quad , \quad i=1,2,\ldots,(n-1) \quad ,$$
$$\delta_o'' = \left(\delta_1 - \delta_o\right) / \ 2\ \delta x_1^2 \quad , \tag{4.9}$$
$$\delta_n'' = \left(\delta_{n-1} - \delta_n\right) / \ 2\ \delta x_1^2 \quad ,$$

for the second derivative. The third derivative was found by applying (4.8) to δ'' calculated from (4.9). This method gave the best results for δ-distributions, and was therefore adopted.

5. RESULTS AND DISCUSSION

The complete computer program was developed in two stages. In the first stage the solution of eqn. (3.1) alone was attempted. This program was tested for the vapor and tube properties for which results are available in [21]. As pointed out in "Introduction", Stack and Merkle solve a much simplified form of (3.1) since besides other simplifications, they use Cartesian coordinates rather than curvilinear coordinates. In fact, we had modified our earlier program to solve Stack and Merkle's equation (14) for the condensate film thickness, and obtained identical results. The finite element program for the solution of eqn. (4.1) was then developed, and the two were coupled.

In the following we present results for one vapor-tube combination for which experimental data is also available [10,11] for comparison. Since our analysis assumes the radius of curvature of the fluted tube to be large compared to the film thickness, it is not realistic to consider sinusoidal flutes with amplitude-to-pitch ratio much above 0.2. With this in mind, we computed results for tube 'F' of Ref. [10,11]. This tube has seven skirts and an I.D. = 22.9 mm. Details of the actual shape of the flute, and its dimensions are not available in [10,11], and were therefore approximated from a blow-up of the tube 'F' photograph in [11]. The relevant fluid (R-113) and tube (aluminum) properties are

$\rho = 1498.343$ kg/m^3 , $\rho_v = 8.58628$ kg/m^3 ,

$\nu = 3.2067 \times 10^{-7}$ m^2/s , $\sigma = 0.01432$ N/m ,

$h_{fg} = 145225.56$ J/kg , $T_s = 325.5$ K ,

$k_f = 0.06951$ W/m-K , $k_w = 205$ W/m-K ,

$T_{woo} = 318.5$ K , $T_c = 318.5$ K (in), 318.8 K (out) ,

$$L = 0.142875 \text{ m} \left(= \frac{46-1}{8} \times \frac{2.54}{100} \right), \quad h_t = 0.88077 \text{ mm},$$

$$P = 1.6141 \text{ mm}, \quad h_o = 0.15543 \text{ mm},$$

where k_f and k_w are the thermal conductivities of the condensate and fluted tube respectively, and h_t and h_o are associated with the flute shape (Fig. 3) taken to be

$$f(x) = h_t + h_o \cos \frac{2\pi x}{P} . \tag{5.1}$$

Thus h_o is half the amplitude of the flute. The fluid properties were calculated at 322 K (mean of T_s and T_{woo}) from known correlations [25]. These values lead to

$$\delta_\gamma = 0.08051 \text{ mm}, \quad x_p = 0.876487 \text{ mm}.$$

After some numerical experimentation involving different step sizes, etc., the solution of eqn. (3.1) was started from $Z_o = 5\times10^{-6}$ with $\beta = 1/2$ (corresponding to central differencing in X), $\delta X = 0.05$, an initial $\delta Z = 5\times10^{-6}$, and an initial $\lambda = 0.5$ (see eqn. (3.5)). Further iteration for the solution of (3.1) was terminated when

$$\left| 1 - \left(\Delta_{i,k}\right)^{m-1} / \left(\Delta_{i,k}\right)^{m} \right| < \varepsilon \text{ for all } i \text{ at every } k , \tag{5.2}$$

where ε was taken to be 10^{-6}. As we marched downstream in the Z-direction, δZ was increased and the relaxation factor λ had to be decreased according to Table 1, which also gives an idea of the number of iterations before (5.2) was

satisfied. Clearly, it takes longer to get the converged solution as we proceed downstream in the Z-direction. Reasons for this will be apparent soon.

Table 1 Some Parameters for Solution of (3.1)

δZ	λ		Z	# of iterations
5×10^{-6}	0.5	up to	0.002	~ 15
8×10^{-6}	0.2	up to	0.01	~ 30
1.25×10^{-5}	0.1	up to	0.0225	~ 50
2×10^{-5}	0.06	up to	0.086	~ 90

Three divisions of the region OABCO (Fig. 3) into finite elements for the solution of eqn. (4.1) were tried. The one selected on the basis of adequate computational accuracy and relatively economical calculation had 154 triangular elements with 108 nodes. There were 11 nodes each on the faces AB, BC, OC and DE (Fig. 3), and 15 nodes on the face AO.

Fig. 9 shows, to true scale, the flute shape (thick curve), and the condensate film shape (dashed curves) at four values of Z = 0.001, 0.01, 0.03, and 0.086. As expected the film thickens quite rapidly in the trough region while it remains thin over the crest. Unfortunately we are unable to present any results for Z much greater than 0.086 since convergence of our solution for the film thickness (with the same tolerance ε) becomes very slow. The principal reason for this slow convergence is the thickening of the film in the trough. Moreover, it is really futile to try to speed-up the convergence

since our formulation for the condensate film thickness is on shaky ground as the film thickens. The non-linear partial differential equation (2.13) comes from a boundary-layer type analysis, i.e., we neglect all velocity gradients except those in the direction normal to the fluted surface. While this is perfectly reasonable over the initial portion of the tube height when the condensate film is thin, it is increasingly questionable as the film thickens in the trough region. It appears that for the fluid-tube combination considered here, it is improper to analyze the film in the trough region in the boundary-layer-sense for $Z > 0.085$. It is also clear from Fig. 10, that shows the absolute value of $d(1/R_1)/dx_1$ at various Z values, that this derivative is negligible in the trough region as compared to its value in the crest region. It is therefore appropriate to neglect the surface tension effects in the trough region once the condensate film has thickened. Fig. 10 also plots the absolute value of the derivative of flute curvature with x_1, and even at the low value of $Z = 0.002$, it is very different from the derivative of condensate-vapor-interface-curvature with x_1.

While these considerations will be undertaken in an extension of this project, it is encouraging to note from Fig. 11 that a linear extrapolation, on a log-log basis, of our results to date shows a fairly good comparison with experimental data. Fig. 11 shows the heat load per half flute (in W) as a function of Z on a log-log scale. The solid portion of the straight line is based on computed results while the dashed portion is the extrapolation. The lone circled point is based on the experimental data [11]. We also checked that heat transfer rates across the faces AB and OC (Fig. 3) matched within 1%. Theoretically they should be identical since faces OA and BC are insulated.

6. SUGGESTIONS FOR FURTHER WORK

Besides the deficiencies mentioned above, our present analysis also neglects the transverse curvature term, i.e., it assumes the film thickness to be small compared to the radius of curvature of the flute. The analysis is therefore restricted, in its present form, to flutes having a small amplitude to pitch ratio. This is, however, a minor drawback since it seems (analytically at least) that we can overcome this deficiency relatively easily. Its implementation in the computer code is yet to be done.

Another assumption, common to all analyses to date, and far more serious in terms of correct modelling of the practical applications, is the complete neglect of vapor shear on the interface. Our code does have the provision for studying its effect but since we have not analyzed the vapor dynamics yet, we simply take the vapor shear to be zero at present. One should also consider the coolant dynamics for a complete solution but all this will undoubtedly be very demanding.

7. REFERENCES

1. Nunn, R. H. and Marto, P. J., "Performance Rating of Enhanced Marine Condensers," NPS Report No. NPS69-82-005, August 1982, 62 pages.

2. Marto, P. J. and Nunn, R. H., "A Critical Review of Heat Transfer Enhancement Techniques for use in Marine Condensers," NPS Report No. NPS69-82-006, September 1982.

3. Williams, A. G., Nandapurkar, S. S., and Holland, F. A., "A Review of Methods for Enhancing Heat Transfer Rate in Surface Condensers," Chem. Engr., Lond., Vol. 233, 1968, pp. CE367-CE373.

4. Gregorig, R., "Hautkondensation an Feingewellten Oberflachen bei Berucksichtigung der Oberflachen-spannungen," Z. Angew. Math. Phys., Vol. V, 1954, pp. 36-49.

5. Lustenader, E. L., Richter, R., and Neugebauer, F. J., "The Use of Thin Films for Increasing Evaporation and Condensation Rates in Process Equipment," J. Heat Transfer, Trans. ASME, Vol. 81, 1959, pp. 297-307.

6. Carnavos, T. C., "Thin-film Distillation," Proc. F. Intern. Symp. on Water Desalination, Paper SWD-17, Washington, 1965.

7. Thomas, D. G., "Enhancement of Film Condensation Heat Transfer Rates on Vertical Tubes by Vertical Wires," Ind. Eng. Chem. Fundamentals, Vol. 6, 1967, pp. 97-103.

8. Thomas, D. G., "Enhancement of Film Condensation Rate on Vertical Tubes by Longitudinal Fins," AIChE. J., Vol. 14, 1968, pp. 644-649.

9. Newson, I. H., and Hodgson, T. D., "The Development of Enhanced Heat Transfer Condenser Tubing," Desalination, Vol. 14, 1974, pp. 291-323.

10. Combs, S. K., "Experimental Data for Ammonia Condensation on Vertical and Inclined Fluted Tubes," Report ORNL-5488, Jan. 1979.

11. Combs, S. K., Mailen, G. S., and Murphy, R. W., "Condensation of Refrigerants on Vertical Fluted Tubes," Report ORNL/TM-5848, Aug. 1978.

12. Edwards, D. K., Gier, K. D., Ayyaswamy, P. S., and Catton, I., "Evaporation and Condensation in Circumferential Grooves on Horizontal Tubes," ASME paper 73-HT-25, 1973.

13. Fujii, T., and Honda, H., "Laminar Filmwise Condensation on a Vertical Single Fluted Plate," Proc. Sixth Intern. Heat Transfer Conf., Toronto, Vol. 2, 1978, pp. 419-424.

14. Mori, Y., Hijikata, K., Hirasawa, S., and Nakayama, W., "Optimized Performance of Condensers with Outside Condensing Surface," in 'Condensation Heat Transfer', (ed.) P. J. Marto and P. G. Kroeger, ASME, 1979, pp.55-62. (Also, J. Heat Transfer, Trans. ASME, Vol. 103, 1981, pp. 96-102).

15. Hirasawa, S., Hijikata, K., Mori, Y., and Nakayama, W., "Effect of Surface Tension on Condensate Motion in Laminar Film Condensation (study of liquid film in a small trough)," Int. J. Heat Mass Transfer, Vol. 23, 1980, pp. 1471-1478.

16. Panchal, C. B., and Bell, K. J., "Analysis of Nusselt-type Condensation on a Vertical Fluted Surface," in 'Condensation Heat Transfer', (ed.) P. J. Marto and P. G. Kroeger, ASME, 1979, pp. 45-53.

17. Panchal, C. B., and Bell, K. J., "Analysis of Nusselt-type Condensation on a Vertical Fluted Surface," Num. Heat Transfer, Vol. 3, 1980, pp. 357-371.

18. Panchal, C. B., and Bell, K. J., "Analysis of Nusselt-type Condensation on a Triangular Fluted Surface," Int. J. Heat Mass Transfer, Vol. 25, 1982, pp. 1909-1911.

19. Barnes, C. G., Jr., and Rohsenow, W. M., "Vertical Fluted Tube Condenser Performance Prediction," Proc. 7th International Heat Transfer Conf., Munich, Vol. 5, 1982, pp. 39-43.

20. Yamamoto, H., and Ishibachi, T., "Calculation of Condensation Heat Transfer Coefficients of Fluted Tubes," Heat Transfer Japanese Res., Vol. 6, 1977, pp. 61-68.

21. Stack, T. G., and Merkle, C. L., "Laminar Filmwise Condensation on a Fluted Vertical Surface," Manuscript.

22. Schlichting, H., "Boundary Layer Theory," McGraw-Hill, 7th Edn., 1979.

23. Ferziger, J. H., "Numerical Methods for Engineering Application," John Wiley & Sons, Inc., 1981.

24. Thompson, J. F. (ed.), "Numerical Grid Generation," North-Holland, 1982.

25. Chapman, R. H., "Saturated Pool and Flow Boiling Studies with Freon-113 and Water at Atmospheric Pressure", ORNL Report No. ORNL-4987, Oak Ridge National Laboratory, Nov., 1974.

APPENDIX A

CURVATURE OF CONDENSATE-VAPOR INTERFACE AND ITS VARIATION ALONG FLUTE SHAPE

Equation (2.13) for the determination of condensate film thickness $\delta(x_1,z)$ involves the value of pressure gradient dp/dx_1 which, in turn, depends upon $d(1/R_i)/dx_1$, as is clear from (2.15). We present below some relations for calculation of this quantity.

The basic terminology is present in Fig. 3, wherein, $f(x)$ denotes the flute shape and $f_i(x)$ the condensate-vapor interface. The position vector to a point on the flute is $\vec{r}_w$, and that to a point on the condensate-vapor interface is $\vec{r}_i$, such that

$$\vec{r}_i - \vec{r}_w = \vec{n}_w \delta \quad , \tag{A.1}$$

where $\vec{n}_w$ is the unit normal to the flute as shown in Fig. 3. We also let x_i be the curvilinear coordinate along the condensate-vapor interface. Then by definition

$$\frac{1}{R_i} \equiv \frac{\partial^2 \vec{r}_i}{\partial x_i^2} \tag{A.2}$$

$$\text{Now } \vec{r}_i = (x, f_i), \tag{A.3}$$

$$\text{and } x_i = \int_0^x (1 + f_i'^2)^{1/2} \, d\zeta \quad , \tag{A.4}$$

where prime denotes differentiation with x. From equation (A.4), we get

$$\frac{dx_i}{dx} = (1 + f_i'^2)^{1/2} \tag{A.5}$$

From (A.3) then

$$\frac{d\vec{r}_i}{dx_i} = \frac{d\vec{r}_i}{dx}\,\frac{dx}{dx_i}$$

$$= (1 + f_i'^2)^{-1/2}\,(1, f_i') \,.$$

Thus

$$\frac{d^2\vec{r}_i}{dx_i^2} = \frac{f_i''}{(1+f_i'^2)^2}\,(-f_i', 1) \,. \qquad \text{(A.6)}$$

From equation (A.2) then

$$\frac{1}{R_i} = \frac{|f_i''|}{(1 + f_i'^2)^{3/2}} \,. \qquad \text{(A.7)}$$

And

$$\frac{d}{dx_1}\left(\frac{1}{R_i}\right) = \frac{d}{dx}\left(\frac{1}{R_i}\right)\frac{dx}{dx_1}$$

$$= \frac{\mathrm{sgn}(f_i'')}{(1+f_i'^2)^{3/2}}\left[f_i''' - 3\,\frac{f_i' f_i''^2}{(1+f_i'^2)}\right]\frac{1}{(1+f'^2)^{1/2}} \,, \qquad \text{(A.8)}$$

since $\dfrac{dx_1}{dx} = (1+f'^2)^{1/2}$ in analogy with (A.5). (A.9)

While equation (A.8) seems to be in a convenient form for calculation of $d(1/R_i)/dx_1$, it is not practical since f_i is known only at a discrete set of unequally-spaced x-values. Thus, finding f_i', f_i'' and f_i''' is troublesome, to say the least. Several attempts to use equation (A.8) had to be abandoned for this reason (see Sec. 4.1 for details).

Another relation for the curvature of the condensate-vapor interface comes from use of equation (A.1), and the fact that the unit normal vector $\vec{n}_w$ is given by

$$\vec{n}_w = \left(-\frac{df}{dx_1}, \frac{dx}{dx_1}\right)$$

$$= (1+f'^2)^{-1/2}(-f', 1) \ . \qquad \text{(A.10)}$$

Thus, from (A.1)

$$\vec{r}_i = \left(x - \frac{\delta f'}{(1+f'^2)^{1/2}} \ , \ f + \frac{\delta}{(1+f'^2)^{1/2}}\right), \text{ since } \vec{r}_w = (x,f).$$

Therefore, $$\frac{d\vec{r}_i}{dx} = \left(1 - \delta' f' - \frac{\delta f''}{(1+f'^2)^{3/2}} \ , \ f' + \delta' - \frac{\delta f' f''}{(1+f'^2)^{3/2}}\right) \ , \qquad \text{(A.11)}$$

where $\delta' \equiv \partial\delta/\partial x_1$ but $f' \equiv df/dx$, etc.. The reason for keeping $\partial\delta/\partial x_1$ in place of $\partial\delta/\partial x$ is that solution of equation (2.13) leads to values of δ at equidistant x_1-values but at non-equidistant x-values. It is therefore convenient to find numerically derivatives of δ with respect to x_1.

Carrying on further, we can find $d^2\vec{r}_i/dx^2$ from (A.11), and then use the relation

$$\frac{1}{R_i} \equiv \frac{\left[|\vec{r}_i'|^2|\vec{r}_i''|^2 - (\vec{r}_i'\cdot\vec{r}_i'')^2\right]^{1/2}}{|\vec{r}_i'|^3} \quad , \tag{A.12}$$

where $\vec{r}_i' = d\vec{r}_i/dx$, to get after some lengthy algebra the expression:

$$\frac{1}{R_i} = \frac{\left|\gamma_5\delta'' + \gamma_4\delta\delta' + \gamma_3\delta + \gamma_2\delta^2 + \gamma_1\,(1-\delta\delta'' + 2\delta'^2)\right|}{\left[\gamma_6(1+\delta'^2) + \gamma_7\delta^2 + \gamma_8\delta\right]^{3/2}} \quad , \tag{A.13}$$

where $\gamma_1 = f''$, $\gamma_2 = \left(\frac{f''}{1+f'^2}\right)^3$,

$\gamma_3 = \frac{-2f''^2}{(1+f'^2)^{3/2}}$, $\gamma_4 = (1+f'^2)^{-1/2}\left(f''' - \frac{3f'f''^2}{1+f'^2}\right)$,

$\gamma_5 = (1+f'^2)^{3/2}$, $\gamma_6 = 1+f'^2$,

$\gamma_7 = \left(\frac{f''}{1+f'^2}\right)^2$, $\gamma_8 = -\frac{2f''}{(1+f'^2)^{1/2}}$.

It is interesting to note that many theoretical analyses that claim to determine the surface tension effect based upon the actual shape of the condensate-vapor interface invariably use

$$\frac{1}{R_i} = \frac{\delta''}{(1+\delta'^2)^{3/2}} \quad , \tag{A.14}$$

for the curvature of the interface. This follows from the correct relation (A.13) if only the first terms in both the numerator and the denominator are retained. However, even for small δ, there is hardly any justification for dropping all other terms in (A.13). The difference between the actual $d(1/R_i)/dx_1$ and that obtained from (A.14) gets further amplified due to differentiation.

For convenience let us write

$$\frac{1}{R_i} = \frac{|N|}{D^{3/2}} = \frac{N.\mathrm{sgn}(N)}{D^{3/2}} \quad ,$$

where the expressions for N and D are clear from equation (A.13). It is then easy to get

$$\frac{d}{dx_1}\left(\frac{1}{R_i}\right) = \frac{\mathrm{sgn}(N)}{D^{3/2}} \Big[\delta'''(\gamma_5 - \delta\gamma_1) + \delta''\{\gamma_5' + \delta(\gamma_4 - \gamma_1') + 3\gamma_1\delta'\} + \gamma_1'$$

$$+ \delta'^2(\gamma_4 + 2\gamma_1') + \delta'\{\gamma_3 + \delta(2\gamma_2 + \gamma_4')\} + \delta^2\gamma_2' + \delta\gamma_3' \Big]$$

$$- \frac{3}{2R_iD}\{\delta'(2\gamma_6\delta'' + 2\gamma_7\delta + \gamma_8) + (1 + \delta'^2)\gamma_6' + \delta^2\gamma_7' + \delta\gamma_8'\}, \tag{A.15}$$

Where

$$\gamma_1' = \frac{d\gamma_1}{dx_1} = f'''(1+f'^2)^{-1/2} \quad ,$$

$$\gamma_2' = \frac{d\gamma_2}{dx_1} = \frac{3f''^2}{(1+f'^2)^{7/2}}\left[f''' - \frac{2f'f''^2}{1+f'^2}\right] \quad ,$$

$$\gamma_3' = \frac{d\gamma_3}{dx_1} = \frac{2f''}{(1+f'^2)^2}\left[\frac{3f'f''^2}{1+f'^2} - 2f'''\right] \quad ,$$

$$\gamma_4' = \frac{d\gamma_4}{dx_1} = \frac{f^{iv}}{1+f'^2} - \frac{f''}{(1+f'^2)^2}(3f''^2 + 7f'f''') + \frac{9f'^2f''^3}{(1+f'^2)^3} \quad ,$$

$$\gamma_5' = \frac{d\gamma_5}{dx_1} = 3f'f'' \quad ,$$

$$\gamma_6' = \frac{d\gamma_6}{dx_1} = 2f'f''(1+f'^2)^{-1/2} \quad ,$$

$$\gamma_7' = \frac{d\gamma_7}{dx_1} = \frac{2f''}{(1+f'^2)^{5/2}}\left(f''' - \frac{2f'f''^2}{1+f'^2}\right) \quad ,$$

and

$$\gamma_8' = \frac{d\gamma_8}{dx_1} = \frac{2}{1+f'^2}\left(\frac{f'f''^2}{1+f'^2} - f'''\right) \quad .$$

Equation (A.15) is quite complicated but as mentioned in the discussion on eqn. (2.13), it contains $\partial^3\delta/\partial x_1^3$. It is therefore essential to determine the condensate film thickness as accurately as possible. Otherwise, errors in finding the third derivative of δ w.r.t. x_1 numerically will be excessive. Due to these numerical difficulties, it was found that use of eqn. (A.15) to find $d(1/R_i)/dx_1$ resulted in mild oscillations in δ-values after a few steps in the Z-direction. Several methods (at least five) were used to find δ-derivatives w.r.t. x_1 but all resulted in oscillatory δ-values; the least oscillations resulted from the use of central-difference formulae.

In order to overcome this difficulty, another relation for $1/R_i$ and its derivative w.r.t. x_1 was developed. This relation, based on eqns. (A.2) and (A.1), is

$$\frac{1}{R_i} = \left| \frac{\partial^2(\vec{r}_w + \vec{n}_w\delta)}{\partial x_i^2} \right|$$

$$= \left| \frac{\partial^2\vec{r}_w}{\partial x_1^2} + \delta\frac{\partial^2\vec{n}_w}{\partial x_1^2} + 2\frac{\partial\vec{n}_w}{\partial x_1}\frac{\partial\delta}{\partial x_1} + \vec{n}_w\frac{\partial^2\delta}{\partial x_1^2} \right| , \qquad (A.16)$$

where $\partial/\partial x_i$ has been approximated by $\partial/\partial x_1$. Noting that $\vec{r}_w = (x,f)$, and $\vec{n}_w$ is given by eqn. (A.10), we get from (A.16), after some algebra, that

$$\frac{1}{R_i} = \left[(\alpha_1 + \alpha_2\delta + \alpha_3\delta' + \alpha_4\delta'')^2 + (\beta_1 + \beta_2\delta + \beta_3\delta' + \beta_4\delta'')^2 \right]^{1/2} , \qquad (A.17)$$

where $\delta' \equiv \partial\delta/\partial x_1$, $f' = df/dx$, etc., and

$$\alpha_1 = -\beta_1 f' \quad ,$$

$$\alpha_2 = \frac{1}{(1+f'^2)^{5/2}} \left(\frac{4f'f''^2}{1+f'^2} - f'''\right) \quad ,$$

$$\alpha_3 = -2\beta_1 \quad ,$$

$$\alpha_4 = -\beta_4 f' \quad ,$$

$$\beta_1 = f''(1+f'^2)^{-2} \quad ,$$

$$\beta_2 = \alpha_2 f' - \beta_1\beta_4 f'' \quad ,$$

$$\beta_3 = 2\alpha_1 \quad ,$$

and $$\beta_4 = (1+f'^2)^{-1/2} \quad .$$

From equation (A.17) it follows that

$$\frac{d}{dx_1}\left(\frac{1}{R_i}\right) = R_i\{(\alpha_1 + \alpha_2\delta + \alpha_3\delta' + \alpha_4\delta'')(\beta_2 + \alpha_2'\delta + 3\alpha_2\delta' - 3\beta_1\delta'' + \alpha_4\delta''')$$

$$+(\beta_1 + \beta_2\delta + \beta_3\delta' + \beta_4\delta'')(-\alpha_2 + \beta_2'\delta + 3\beta_2\delta' + 3\alpha_1\delta'' + \beta_4\delta''')\} \quad , \quad (A.18)$$

where

$$\alpha_2' = \frac{d\alpha_2}{dx_1} = \frac{1}{(1+f'^2)^3} \frac{f''(4f''^2 + 13f'f''')}{1 + f'^2} - f^{iv} - \frac{28f'^2f''^3}{(1+f'^2)^2} ,$$

and

$$\beta_2' = \frac{d\beta_2}{dx_1} = \alpha_2 f' + f''(2\beta_4\alpha_2 - \alpha_1\beta_1) - \beta_1\beta_4^2 f''' .$$

Equation (A.18) also contains $\partial^3\delta/\partial x_1^3$, but unlike equation (A.15), it yields stable (non-oscillatory) values of δ upon integration of eqn.(2.13). This relation was therefore used in the final computer code.

APPENDIX B

Nonlinear Equations Solution by Newton-Raphson Method

Consider the set of equations

$$[K]\{x\} = \{R\}$$

or $$\sum_{j=1}^{n} k_{ij}(x_1, x_2, .., x_n)x_j = R_i(x_1, x_2, .., x_n) \quad , i = 1, 2, .., n.$$

where k_{ij} and R_i are non-linear functions of $x_1, x_2, .., x_n$.

Let $F_i(x_1, x_2,.., x_n) = \sum_{j=1}^{n} k_{ij}(x_1, x_2, .., x_n)x_j - R_i(x_1, x_2, .., x_n)$,

$$i = 1, 2, .., n.$$

So F_i is the residue in the i^{th} eqn. For solution $F_i = 0$, $i = 1, 2, .., n$. Expanding F_i by Taylor series, we write

$$F_i(x_1 + \Delta x_1, x_2 + \Delta x_2, .., x_n + \Delta x_n)$$

$$= F_i(x_1, x_2, .., x_n) + \sum_{j=1}^{n} \frac{\partial F_i}{\partial x_j}(x_1, x_2, .., x_n)\Delta x_j + \ldots,$$

$$i = 1, 2, .., n.$$

Neglecting all higher-order terms and setting leftside = 0 for a solution, we get

$$\sum_{j=1}^{n} \frac{\partial F_i}{\partial x_j}(x_1, x_2, .., x_n)\Delta x_j = -F_i(x_1, x_2\ldots, x_n) \quad , \quad i = 1, 2, .., n.$$

Thus Newton-Raphson iteration algorithm can be written as

$$[J]^m \{\Delta x\}^{m+1} = -\{F\}^m$$

$$\{x\}^{m+1} = \{x\}^m + \{\Delta x\}^{m+1}$$

where m denotes m^{th} iteration & $[J]^m$ is the system Jacobian at the m^{th} iteration.

The elements of $[J]^m$ are

$$J_{ij}^m = \frac{\partial F_i}{\partial x_j} (x_1^m , x_2^m , \ldots , x_n^m) .$$

If it is too time consuming to compute $[J]^m$ at every iteration, find [J] once and use it until convergence, which will be slow, however.

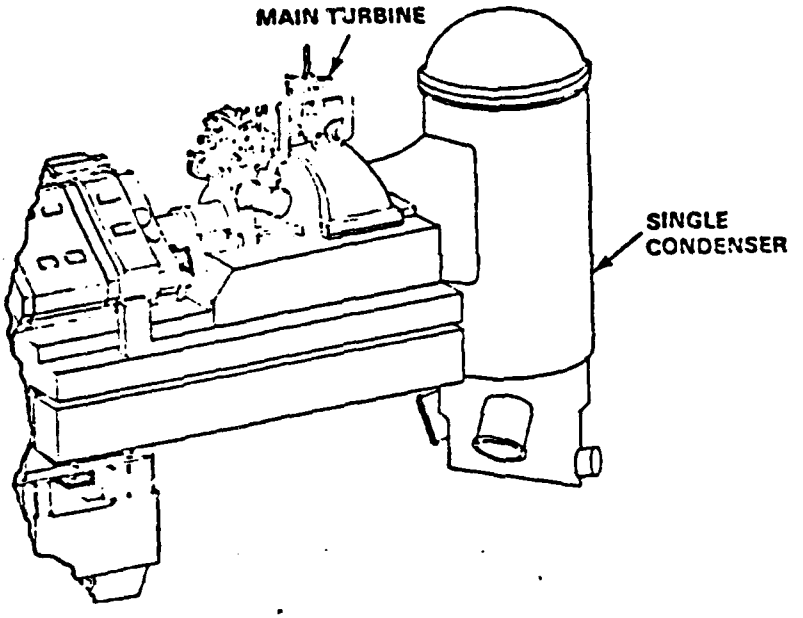

(a) Condenser arrangement

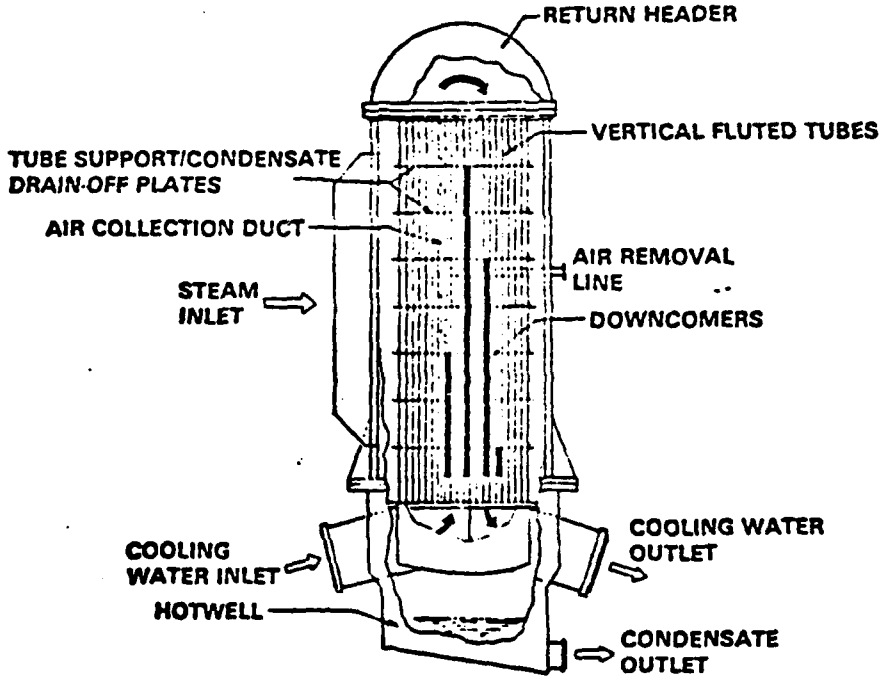

(b) Cross section of vertical condenser.

Fig. 1. Vertical Submarine Condenser

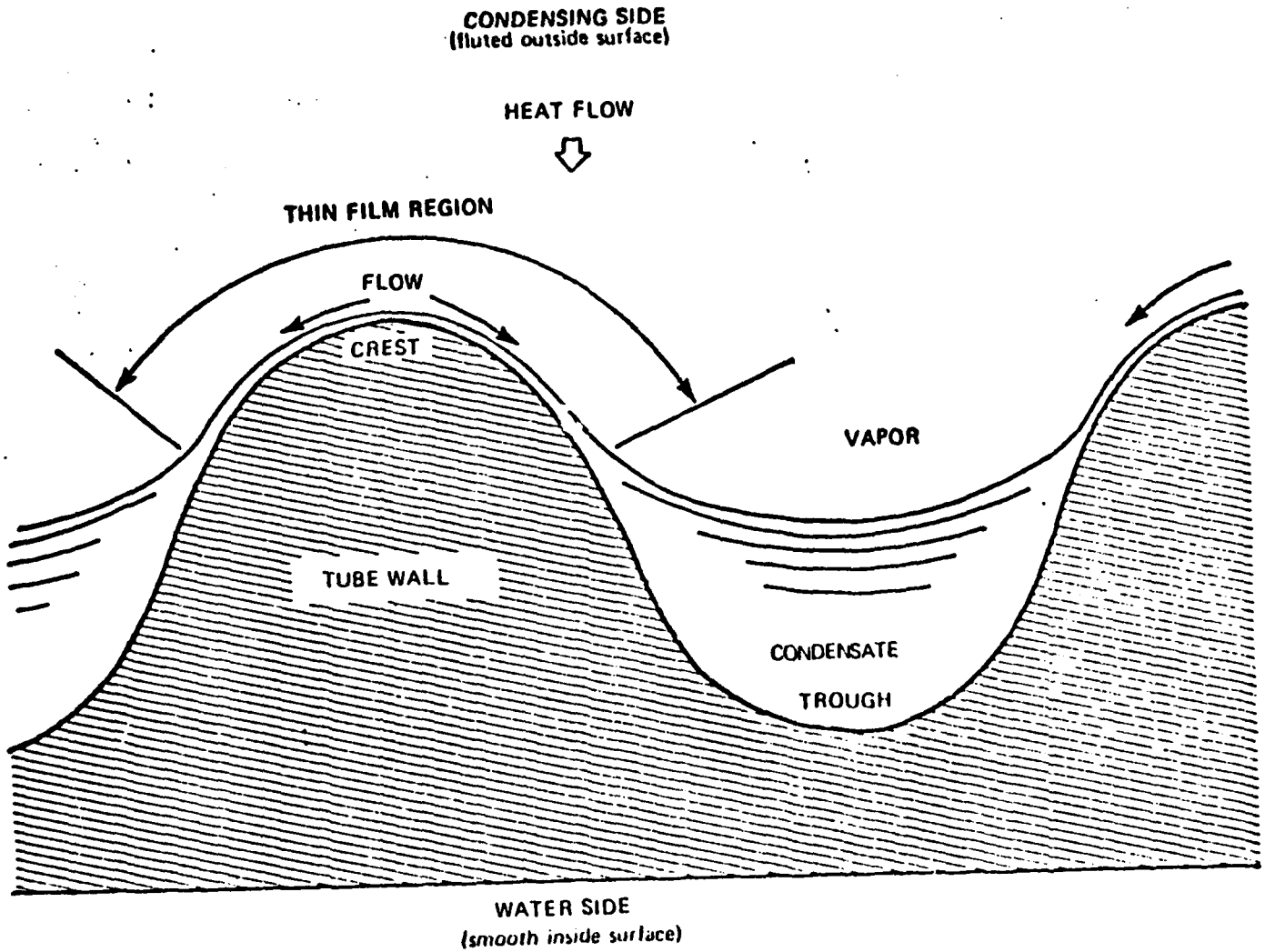

Fig. 2. Fluted tube principle of operation (condensation mode) — surface tension forces acting to push condensate from crests into troughs.

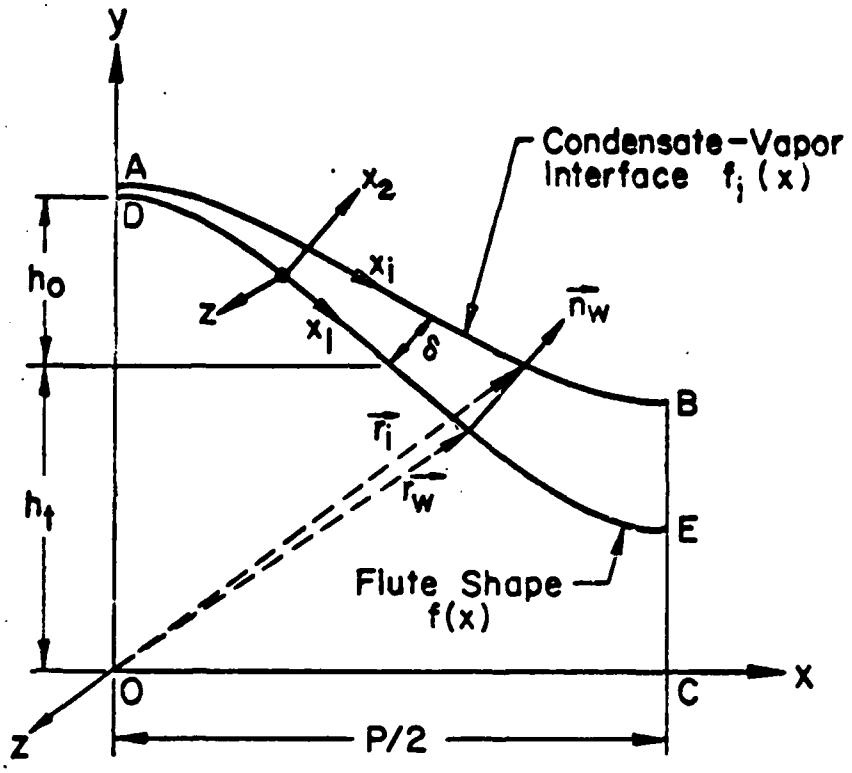

Fig. 3 Co-ordinate System.

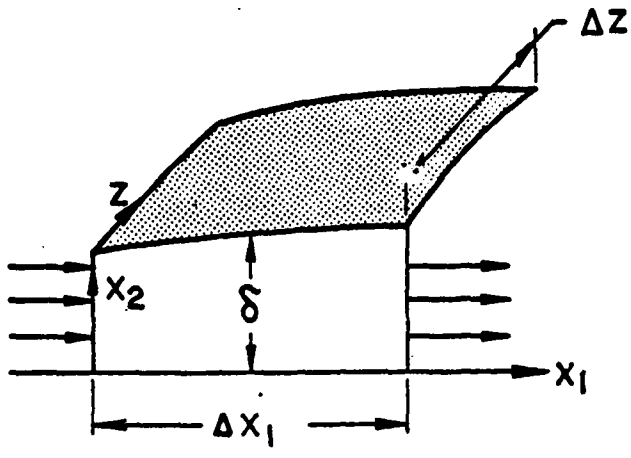

Fig. 4 Control Volume in the Condensate Film.

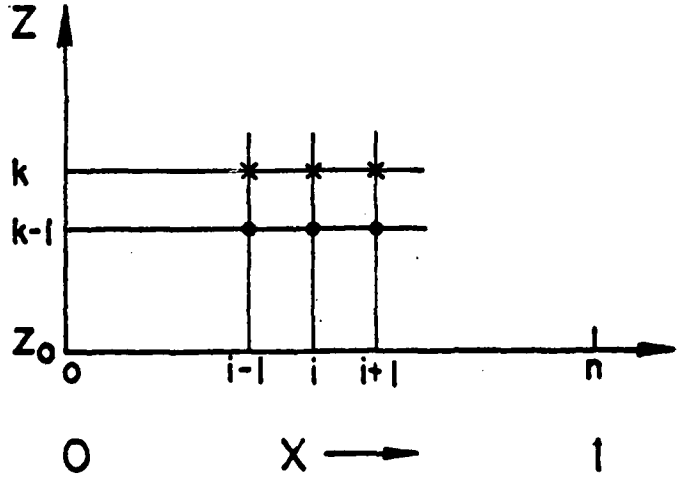

FIG. 5 Finite Difference Grid.

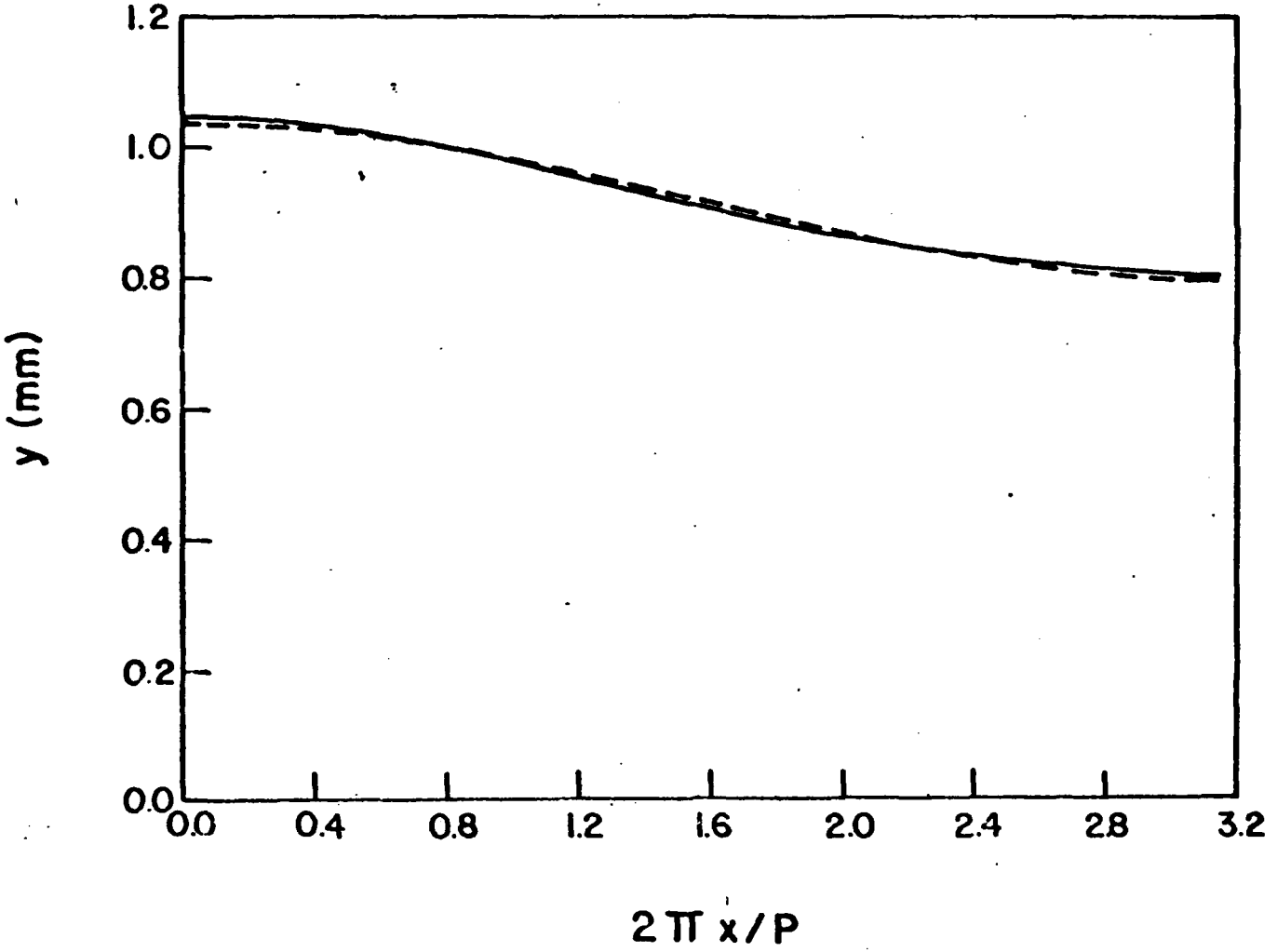

Fig. 6 One Cosine Fit (---) Over the Entire Condensate-Vapor Interface (—) at $Z \simeq 0.08$.

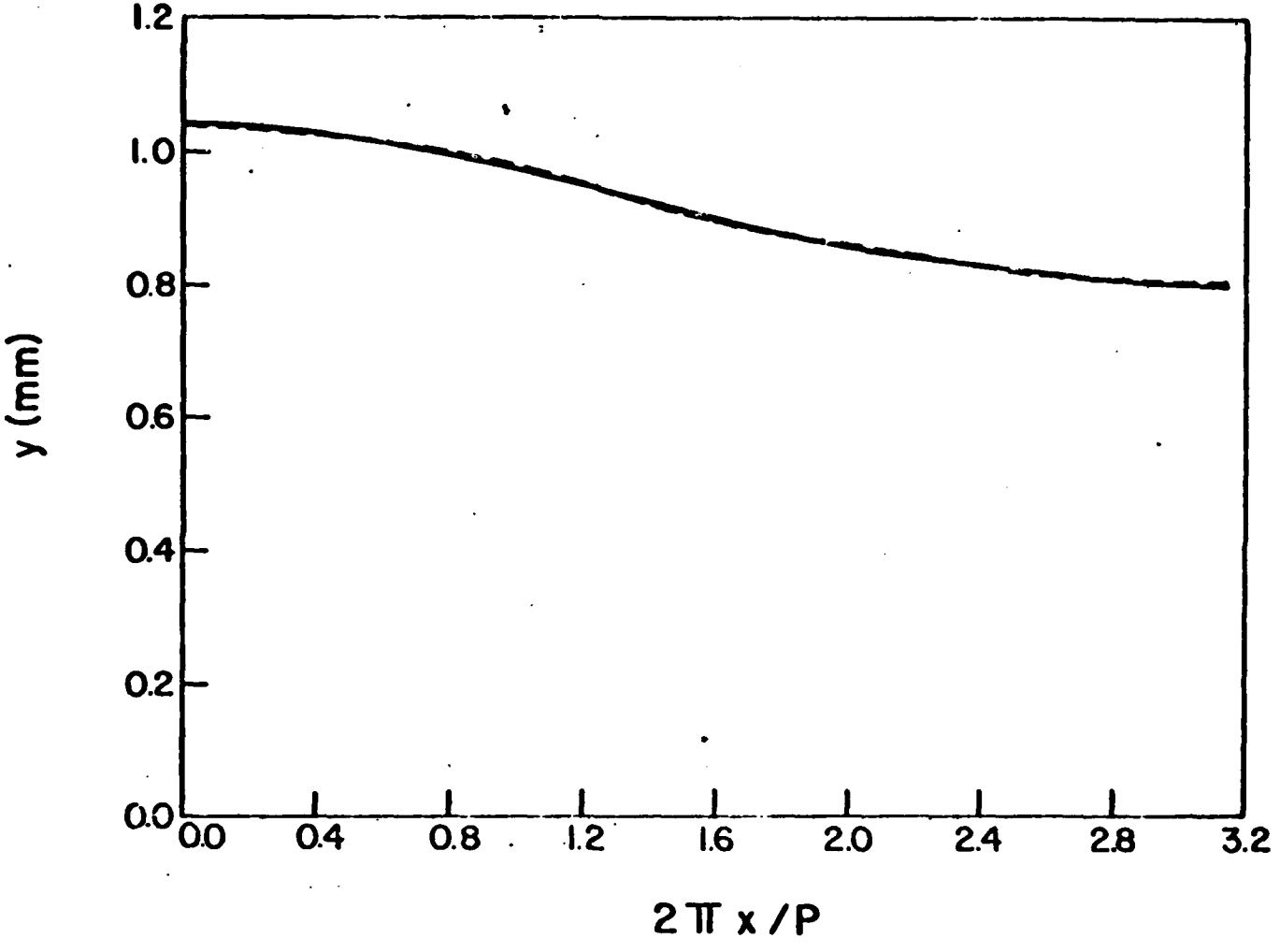

Fig. 7 Two Cosine Fits (---) Over the Condensate-Vapor Interface (—) at $Z \simeq 0.08$.

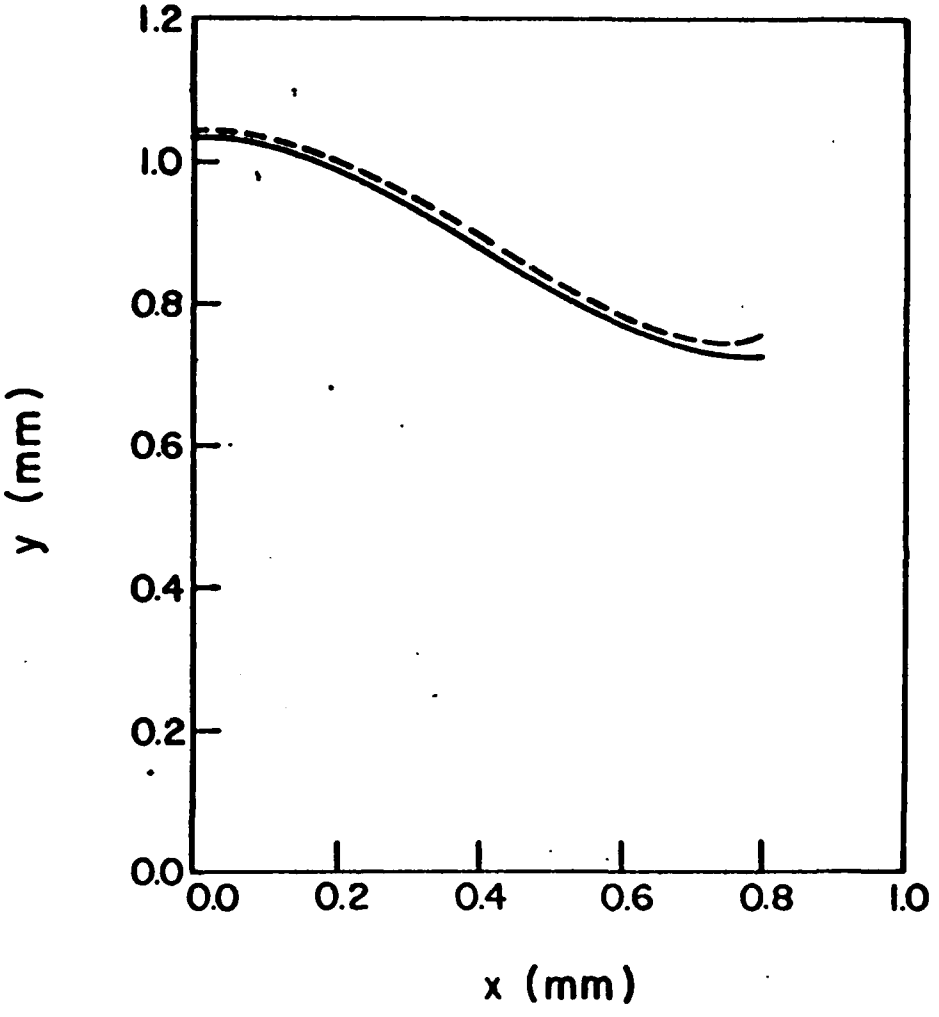

Fig. 8 Flute Shape (—) and an Erroneous Film Shape at Some Z .

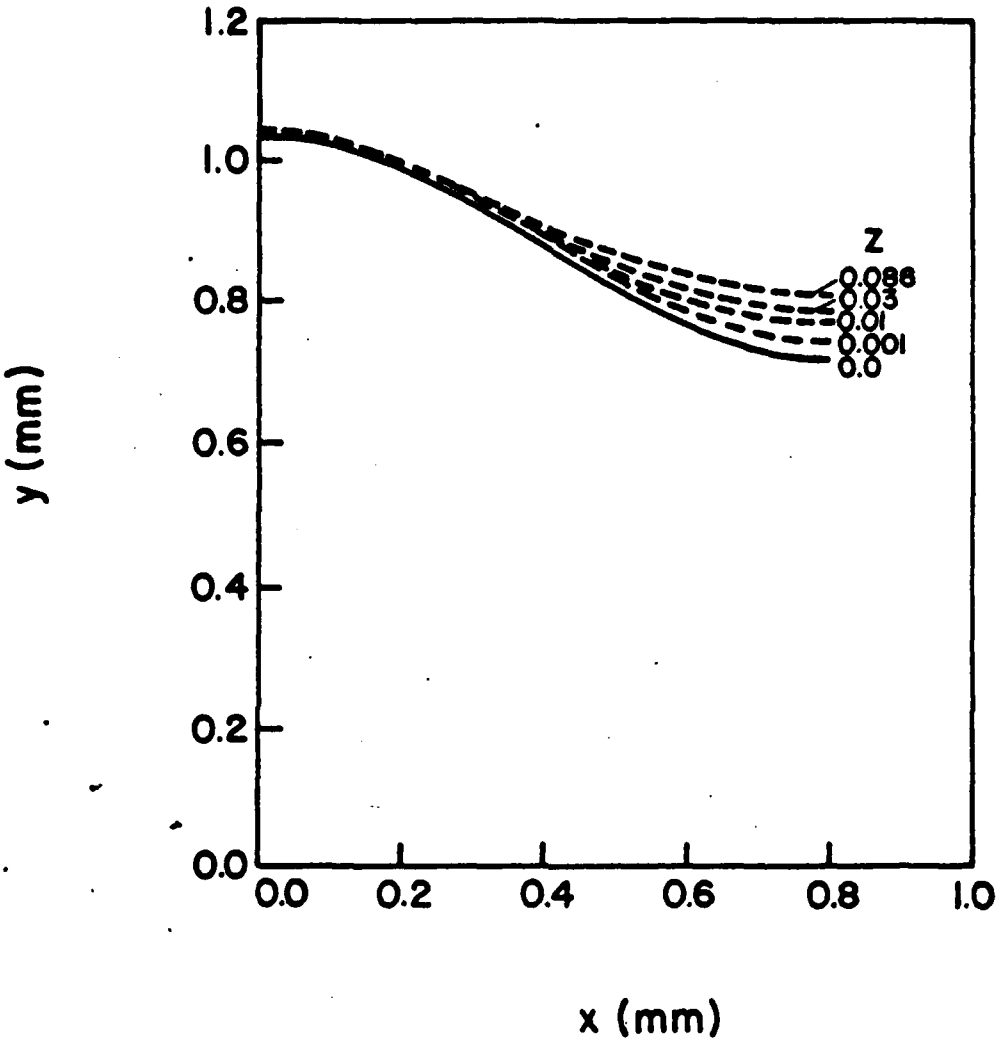

Fig. 9 Flute Shape (—) and Correct Film Shapes at Some Z Locations.

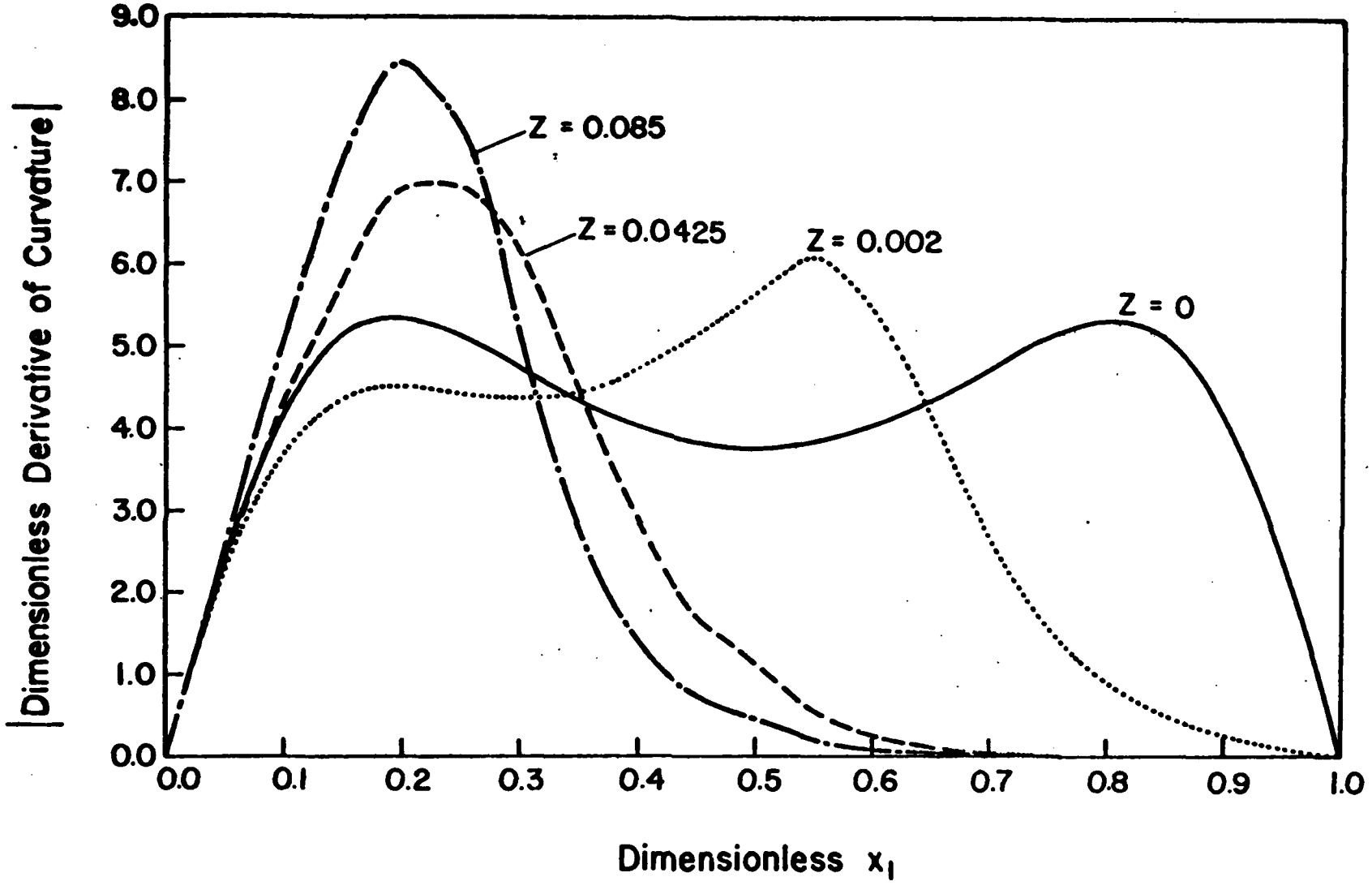

Fig. 10 Comparison of Dimensionless Derivative of the Curvature of Flute (—) and Condensate - Vapor Interface at Various Z Values.

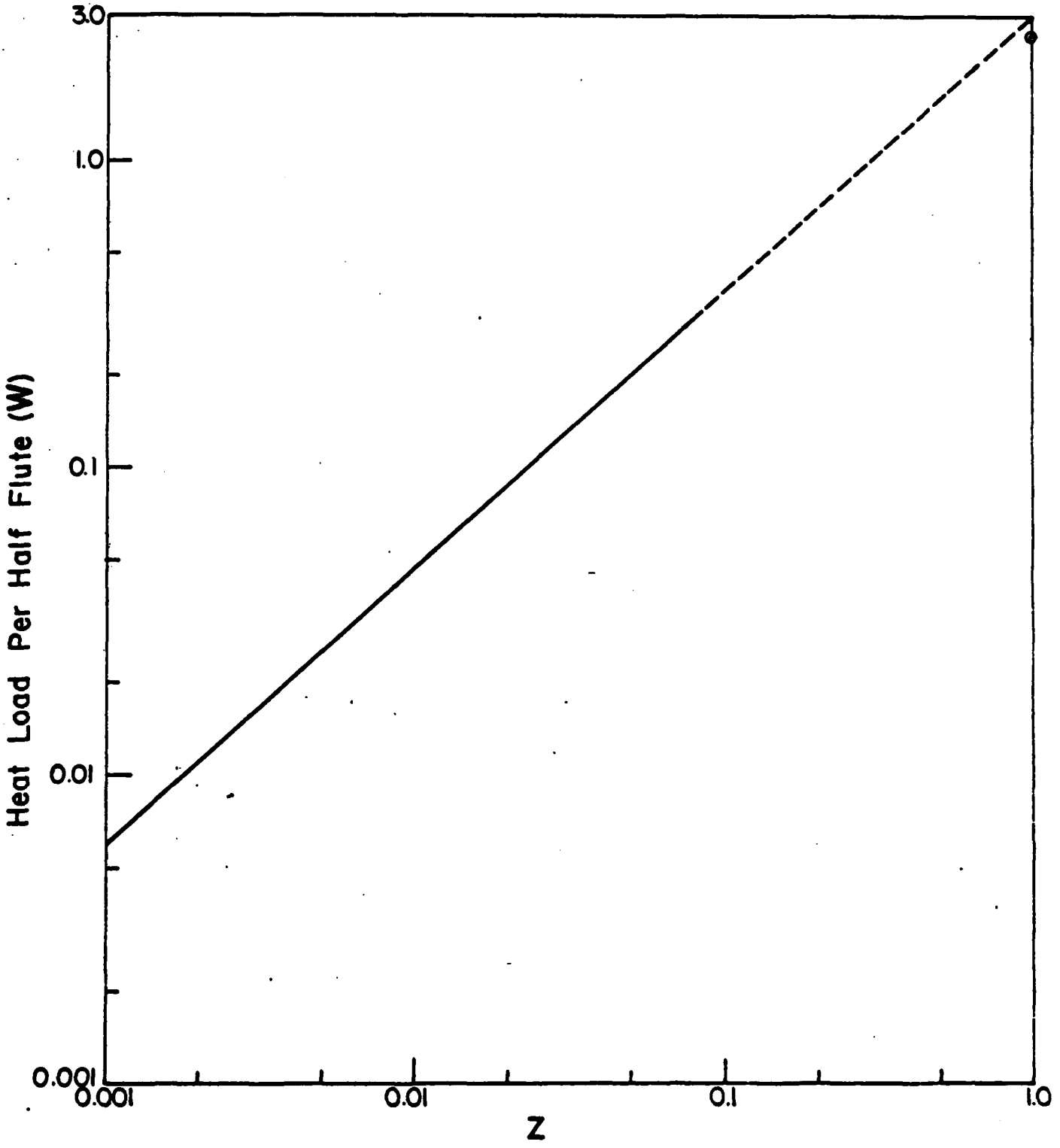

Fig. 11. Heat Load (in W) as a Function of Z .—, Computed; ----, Extrapolated; ⊙, Experimental [11]

INITIAL DISTRIBUTION LIST

		Number of Copies
1.	Defense Technical Information Center Cameron Station Alexandria, VA 22314	2
2.	Library, Code 0142 Naval Postgraduate School Monterey, CA 93943	2
3.	Office of Research Administration, Code 012 Naval Postgraduate School Monterey, CA 93943	1
4.	Professor P. J. Marto, Code 69Mx Department of Mechanical Engineering Naval Postgraduate School Monterey, CA 93943	5
5.	Professor V. K. Garg Department of Mechanical Engineering Indian Institute of Technology Kanpur 208 016 INDIA	3

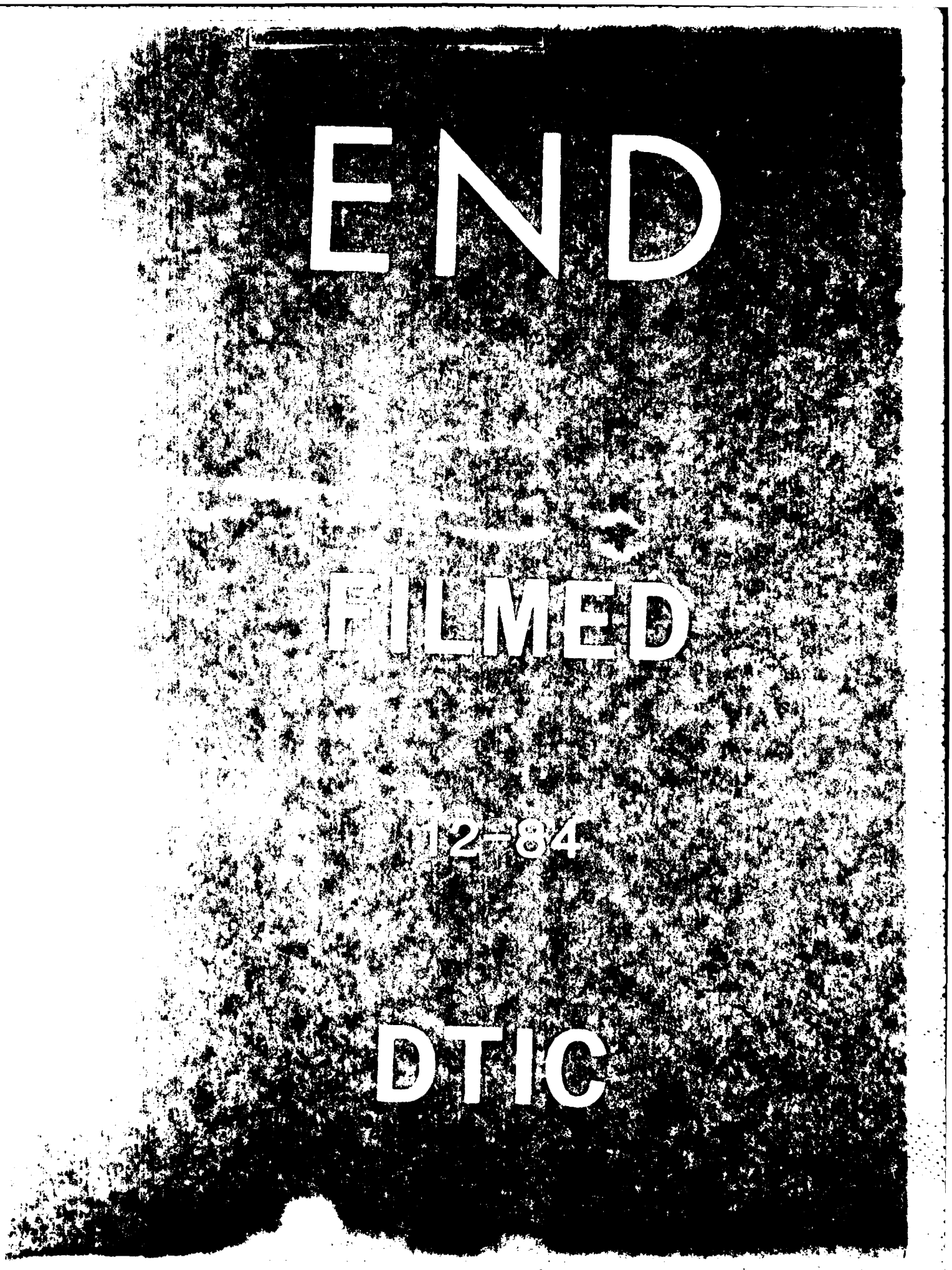
END
FILMED
12-84
DTIC